7.0 Results

The objective of this research is to develop tools that help the designer in visualizing the error between two matching surfaces. Typically, effective visualization entails reduction of data related to the error and graphical presentation of the data. The methodology utilized for achieving this abstraction has been discussed in earlier sections. Matlab (version 5.3) is used in this research for implementation of these methods as well as graphical presentation of the abstracted information. This section presents some of the results obtained from applying these methods. The trimmed or matching surface for a given patch is simulated by modifying the geometry locally. The manipulation of the geometry for these tests and the subsequent data collection has been achieved using two popular CAD software – Dassault Systeme's CATIA (version 4.0) and SDRC's I-DEAS (version 6.0).

A model of part of the bumper of a Porsche 930 has been used in this research for achieving the desired geometry modification. Figures 7.1 and 7.2 show the model of the car rendered in color and as a wireframe respectively. Figure 7.3 shows the part oriented in 3-D space. A grid of 21 × 21 points (corresponding to a 5% or 0.05 increment in the parameter value in either direction) has been used to sample data on the part. This

sampling rate was found to be fine enough to catch or trap even small changes to geometry. The following paragraphs will describe the results obtained from applying these methods to a number of test cases.

The first case (referred to as case (i)) illustrates the differences between two surfaces that are matched perfectly except for a small area of defect. Figure 7.4 shows the error surface mapped on to the *u, v* parametric plane. As the reader can see, the two surfaces are perfectly matched, except for a small area of localized defect. The reader should note that the error surface is mapped on to the parametric plane and this figure does not represent the actual dimensions of the patch. Table 7.1 compares the magnitude of the defect to the dimensions of the bounding box for the original patch. Figure 7.5 shows the area on the parametric plane corresponding to error greater than 5% of the maximum error for the matching patch. Figures 7.6 and 7.7 show the line fits to the data along individual isoparametric curves in both *u* and *v* parametric direction. The absolute value of the ordinate values for each of these fits is plotted against the parameter value to obtain a plot that replicates the shape of the original error surface. Figures 7.8 and 7.9 present the ordinate plots in either parametric direction.

Case (ii) presents results for the error between a pair of matching surfaces with two areas of localized discrepancy. Figures 7.10 through 7.13 show the error surface, areas on surface with significant position discrepancy, and the ordinate plots for a matching surface with two areas of deformity. Again, the criterion for selection of significant position error is taken to be greater than 5% of the maximum error for the patch.

Notice that the ordinate plots successfully reduce the data successfully and convey useful information about the matching surface in terms of magnitude and location of discrepancy. However, due to the data being sampled at only a number of points on the surface, the resolution of the error shape obtained from the ordinate plot is not very good. This is a problem inherent to the discretization process. An attempt is made to give the reader a flavor of increased resolution in case (iii) with three areas of discrepancy on the matching surface. Figures 7.14 through 7.17 illustrate this case.

The ordinate plot is not only a good qualitative measure of error between two matching surfaces, but it can also be employed to gain quantitative information about two matching surfaces. The correlation between points of maximum error on a patch and the value of the ordinates on the plot has been investigated. Tables 7.2 through 7.4 present the results of this investigation for the three cases of matching surfaces discussed above.

However, note that predicting the location of discrepancies by just glancing at two plots (one in either direction) is the main purpose of the above data reduction and presentation. The correlation and the subsequent estimation merely demonstrate the efficacy of the method. The reader will notice that even though the correlation between maximum values of error and the ordinate intercept values is high for all cases, it does fluctuate from case to case. This is an obvious limitation of data reduction. To understand the implications of the above statement, consider the fact that the ordinate intercept value from a linear least square fit attempts to model the characteristic behavior of all the points

sampled on that isoparametric curve. However, it is a fact that the model will not represent every point on the curve with the same veracity. Therefore, it follows that even though the ordinate intercept values obtained from the linear least squares fit seem to be a good measure of the error between two surfaces, they do not accurately model the error magnitude at every single point.

Table 7.1: Table comparing the maximum error magnitude to the dimensions of the bounding box for the original patch. All units in mm.

The dimension of the bounding box along x axis	513.935
The dimension of the bounding box along y axis	924.307
The dimension of the bounding box along z axis	303.08
The magnitude of maximum error	0.214181
Error magnitude as % of bounding box dimension along x axis	0.0416747
Error magnitude as % of bounding box dimension along y axis	0.0231721
Error magnitude as % of bounding box dimension along z axis	0.0706681

Table 7.2: Case (i) - Table showing the correlation between the ordinate values and the maximum value of error in both u and v directions. All units in mm.

The magnitude of maximum error	0.214181
Results along u parametric direction	
Correlation coefficient between 21 maximum values of error and ordinate values	0.999403
The predicted value of maximum error	0.213806
Percentage error between actual and predicted value	0.175233
Results along v parametric direction	
Correlation coefficient between 21 maximum values of error and ordinate values	0.963788
The predicted value of maximum error	0.216634
Percentage error between actual and predicted value	-1.14531

Table 7.3: Case (ii) - Table showing the correlation between the ordinate values and the maximum value of error in both u and v directions. All units in mm.

The magnitude of maximum error	0.856753
Results along u parametric direction	
Correlation coefficient between 21 maximum values of error and ordinate values	0.852043
The predicted value of maximum error	0.968905
Percentage error between actual and predicted value	-13.0904
Results along v parametric direction	
Correlation coefficient between 21 maximum values of error and ordinate values	0.897234
The predicted value of maximum error	1.00254
Percentage error between actual and predicted value	-17.0168

Table 7.4: Case (iii) - Table showing the correlation between the ordinate values and the maximum value of error in both u and v directions. All units in mm.

The magnitude of maximum error	0.414148
Results along u parametric direction	
Correlation coefficient between 21 maximum values of error and ordinate values	0.867258
The predicted value of maximum error	0.478665
Percentage error between actual and predicted value	-15.578
Results along v parametric direction	
Correlation coefficient between 21 maximum values of error and ordinate values	0.796881
The predicted value of maximum error	0.508281
Percentage error between actual and predicted value	-22.791

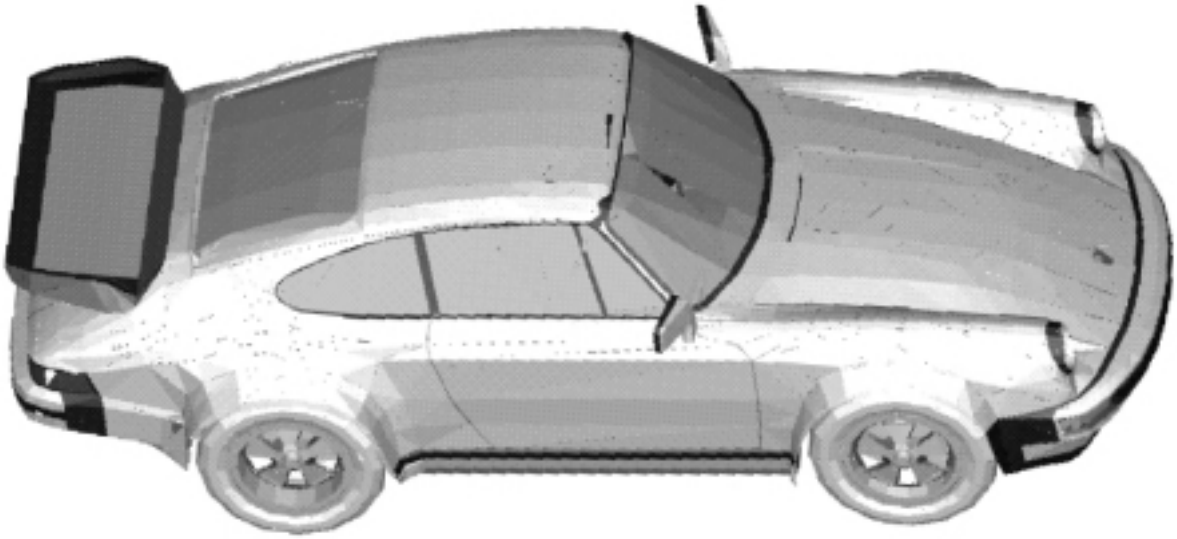

Figure 7.1: Model of a Porsche 930. A part of the front bumper from this model has been used in this research.

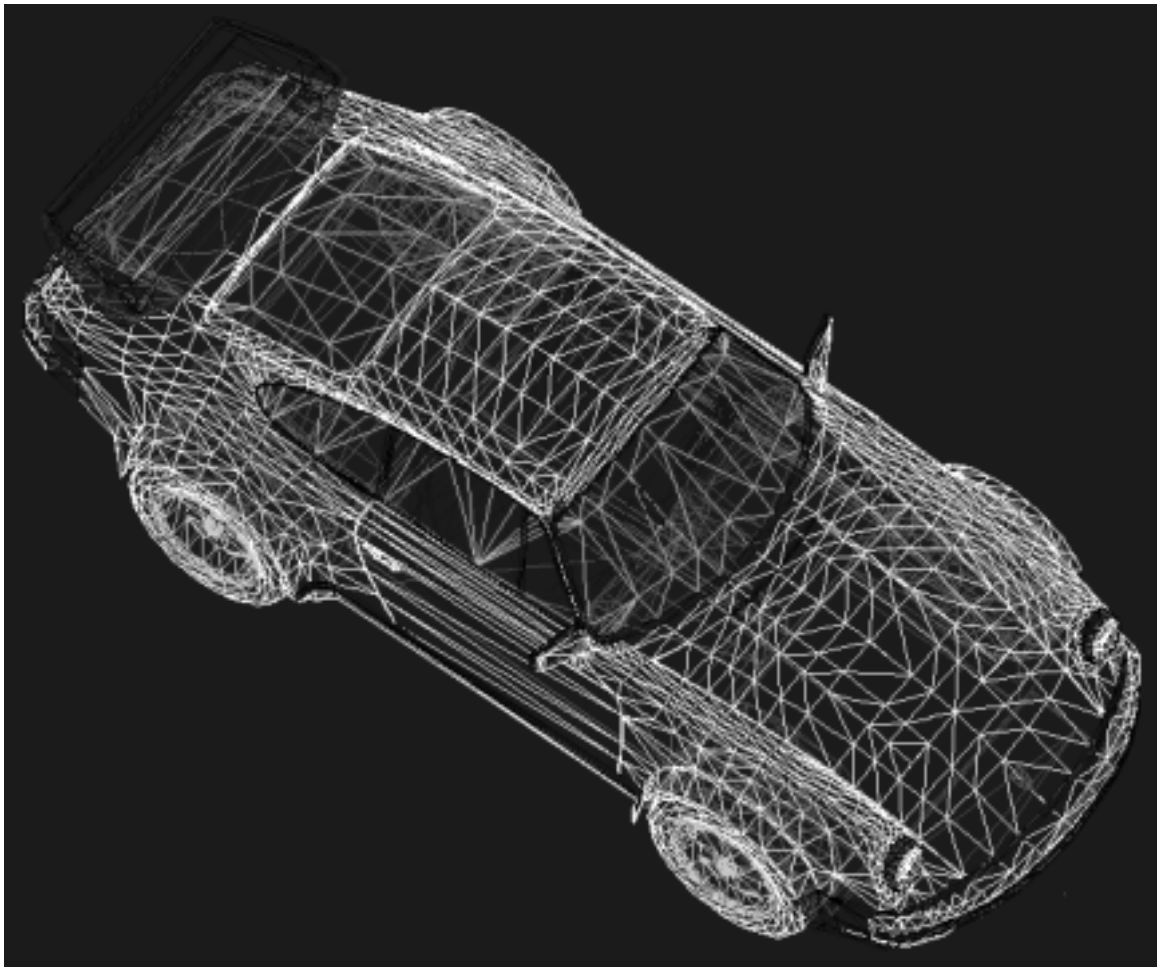

Figure 7.2: Wireframe representation of the above model with hidden line removal enabled.

Figure 7.3: Part of the bumper of a Porsche 930 shown in cartesian space.. This part has been used for the geometry modifications and manipulations in this research.

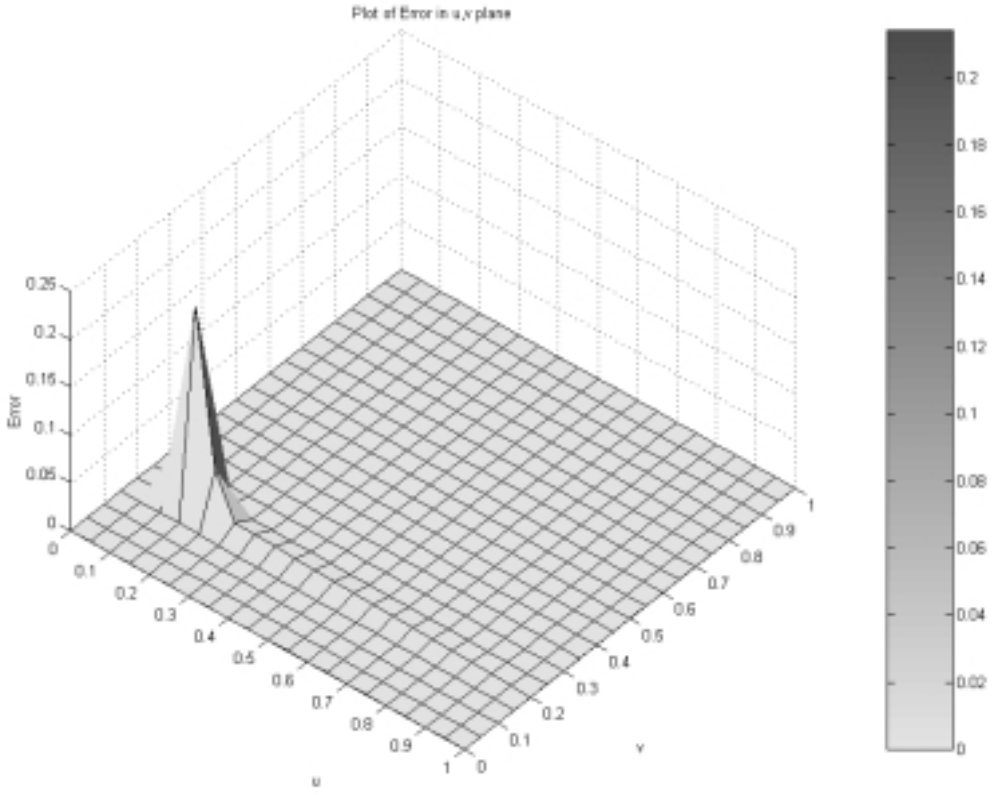

Figure 7.4: Case (i) - Error surface mapped to the parametric plane. The bar on the left maps the error on the surface to the color of the rendered image.

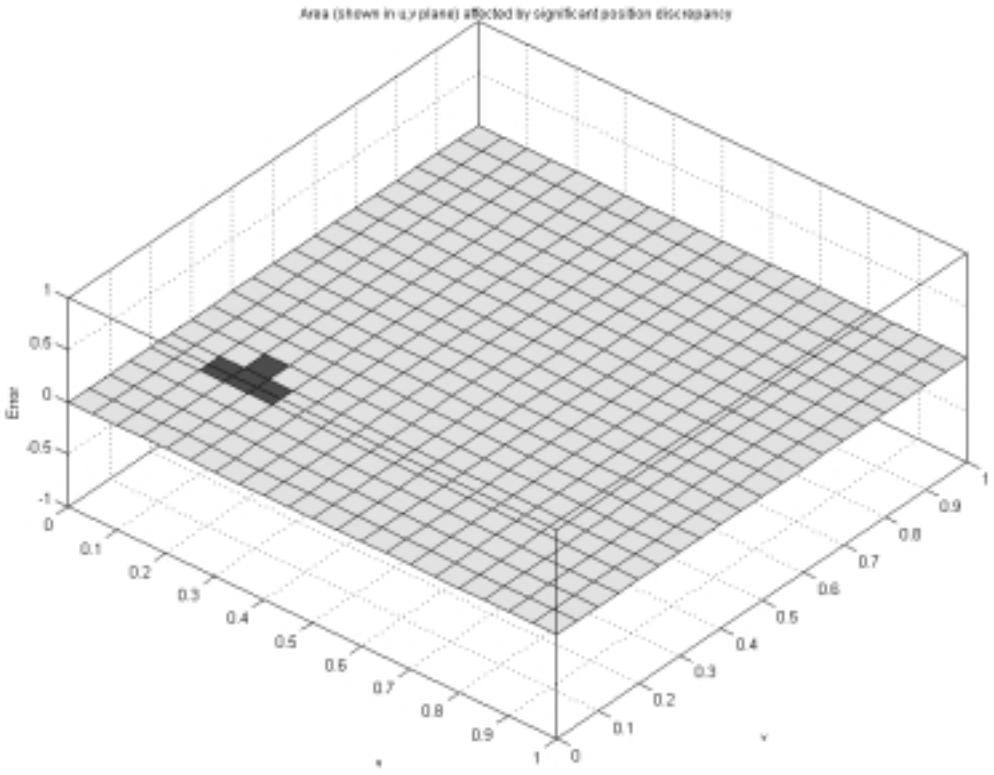

Figure 7.5: Case (i) - Area on the error surface having significant position discrepancy (greater than 5% of maximum error).

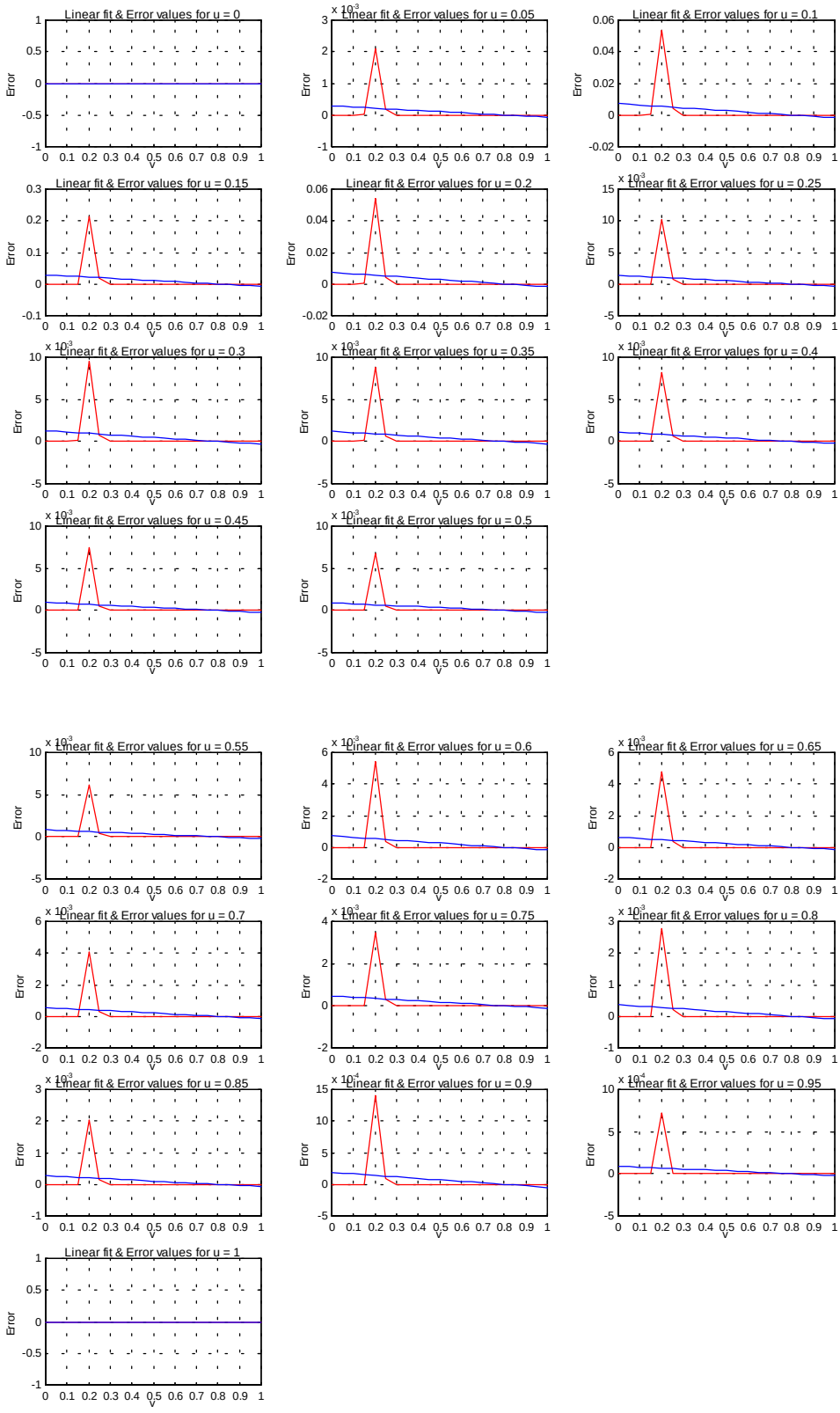

Figure 7.6: Case (i) - Error data taken at isoparametric lines along u direction and the corresponding linear fits.

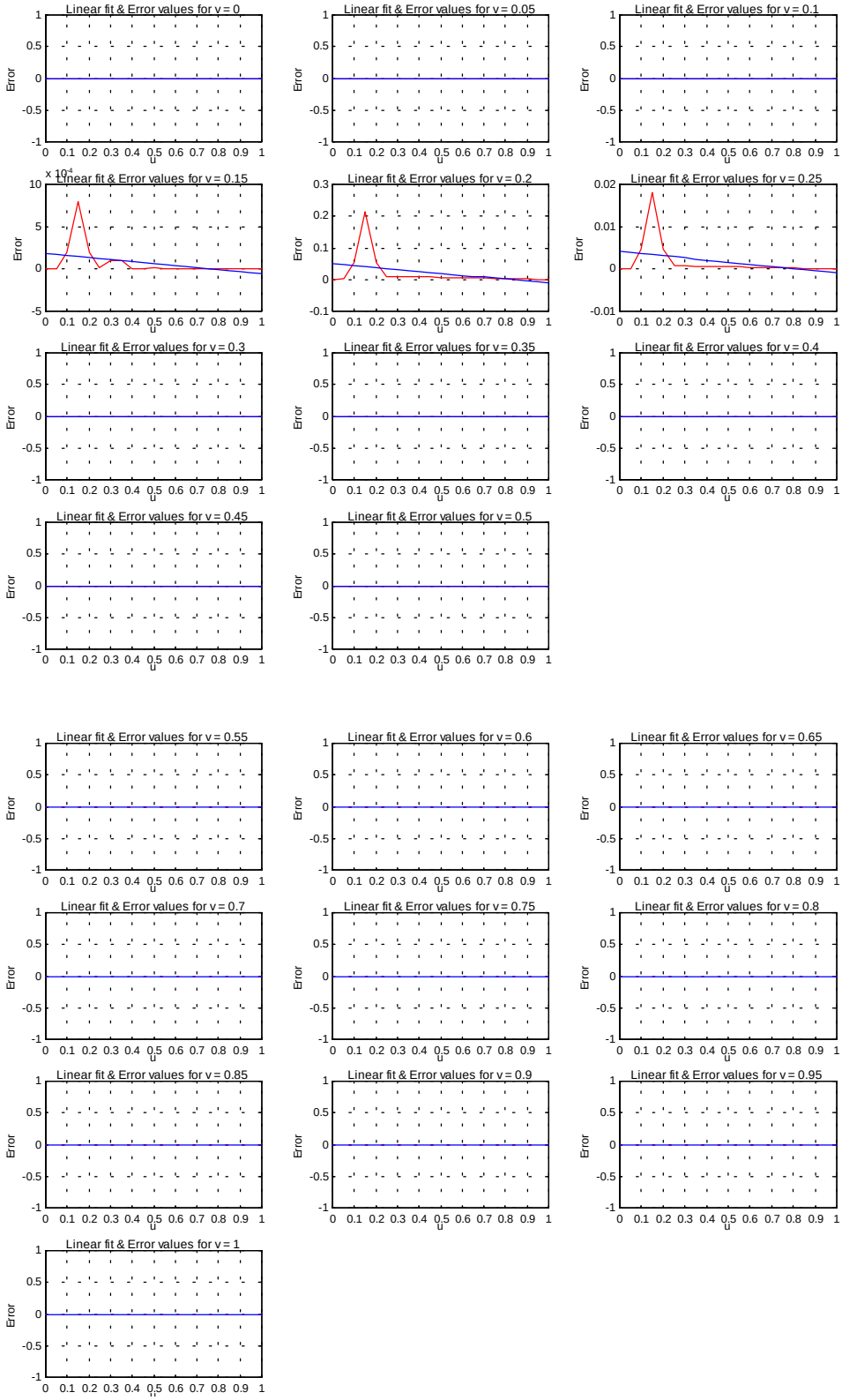

Figure 7.7: Case (i) - Error data taken at isoparametric lines along v direction and the corresponding linear fits.

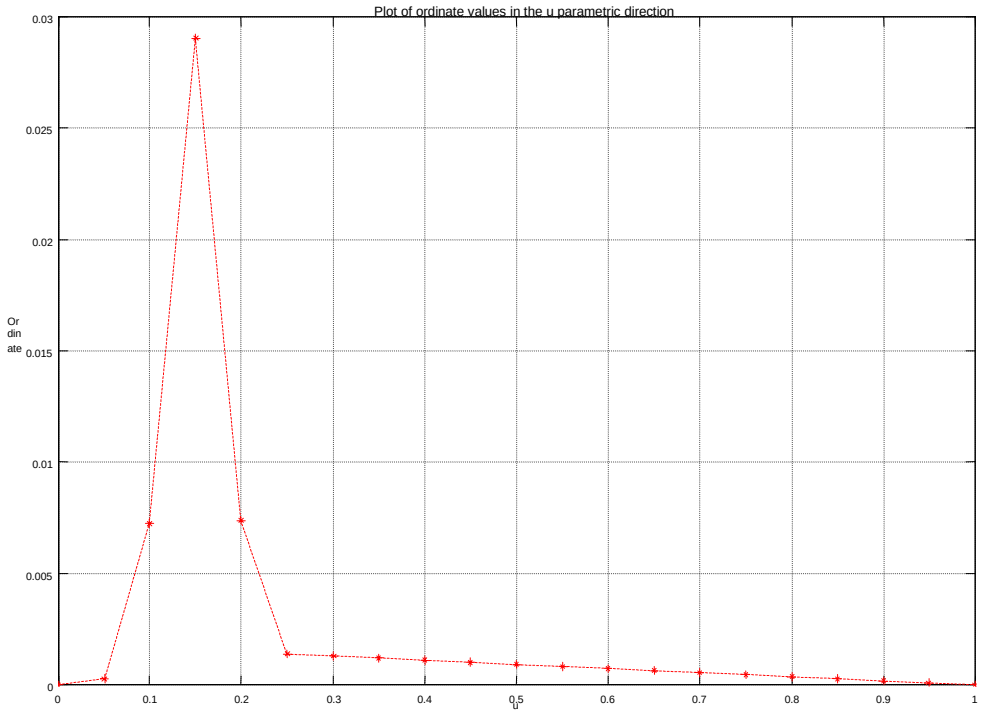

Figure 7.8: Case (i) - Ordinate plot in the u direction replicating the shape of the error surface in that direction.

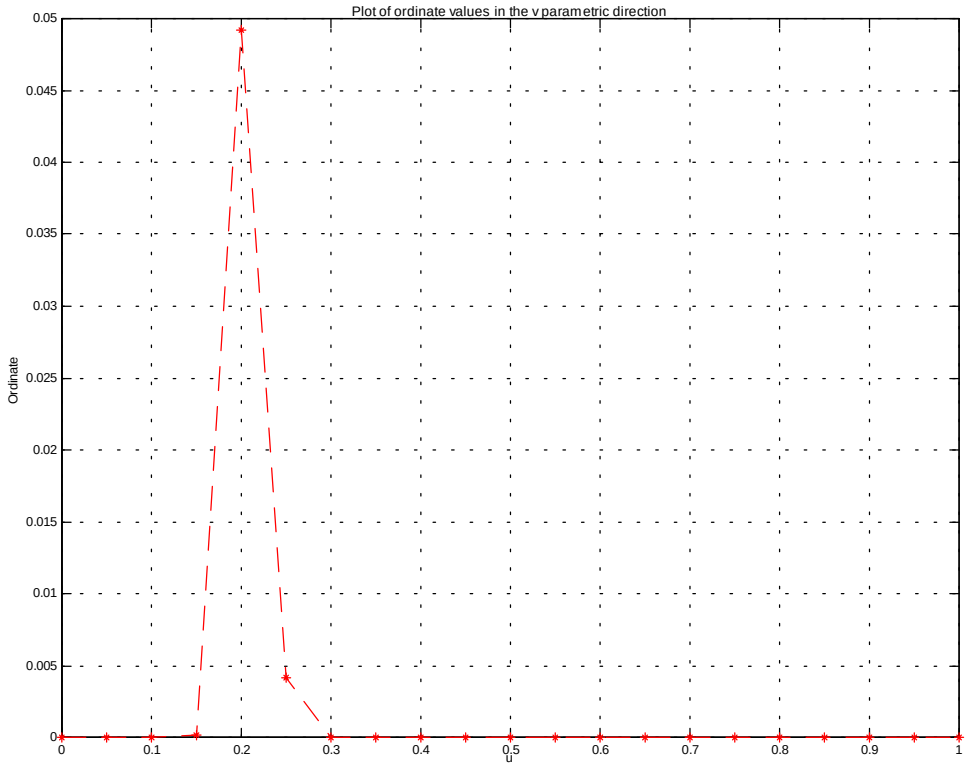

Figure 7.9: Case (i) - Ordinate plot in the v direction replicating the shape of the error surface in that direction.

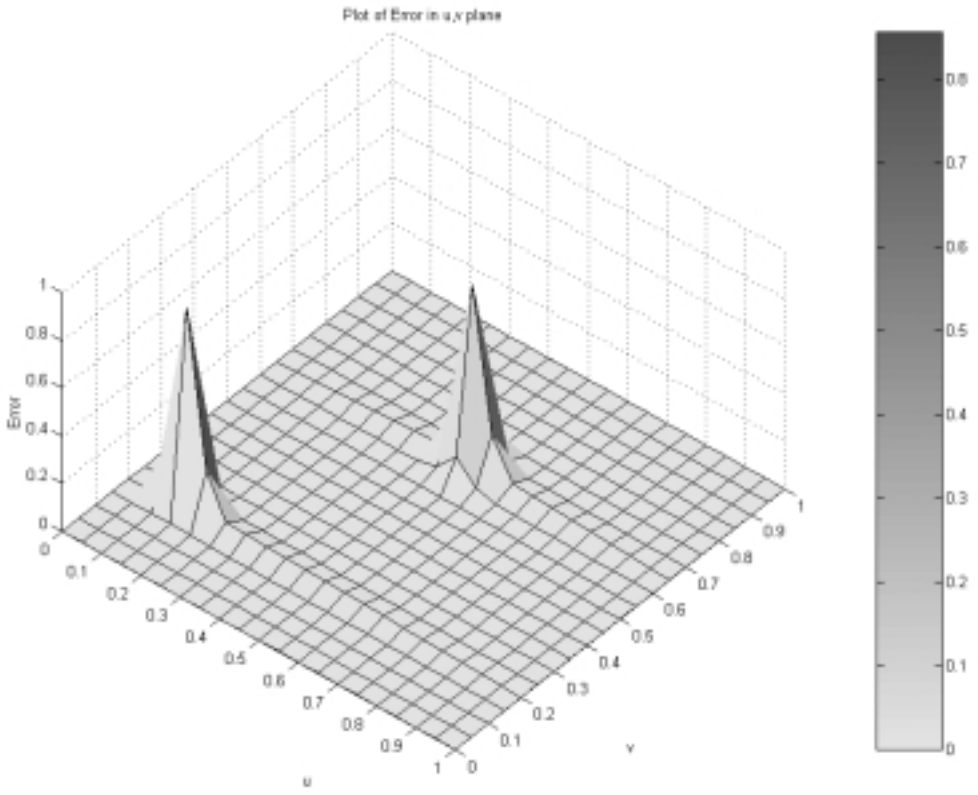

Figure 7.10: Case (ii) - Error plot in parametric plane with two areas of deformity. The bar on the left color codes the magnitude of the error.

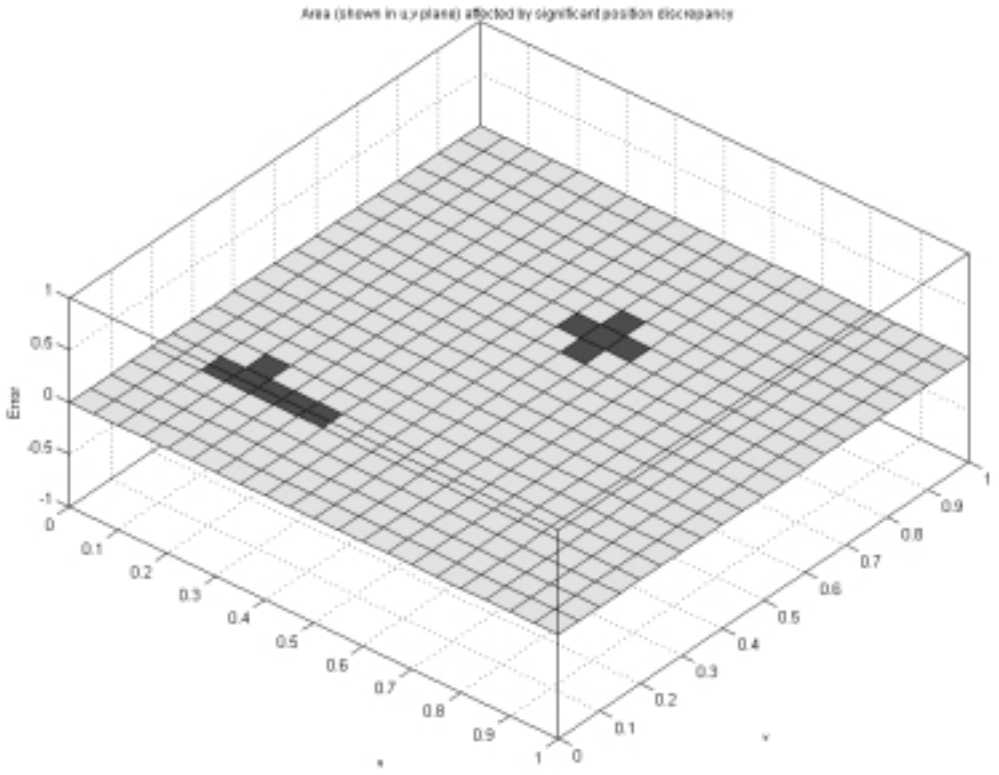

Figure 7.11: Case (ii) - Areas on the above error surface with significant position error marked in red.

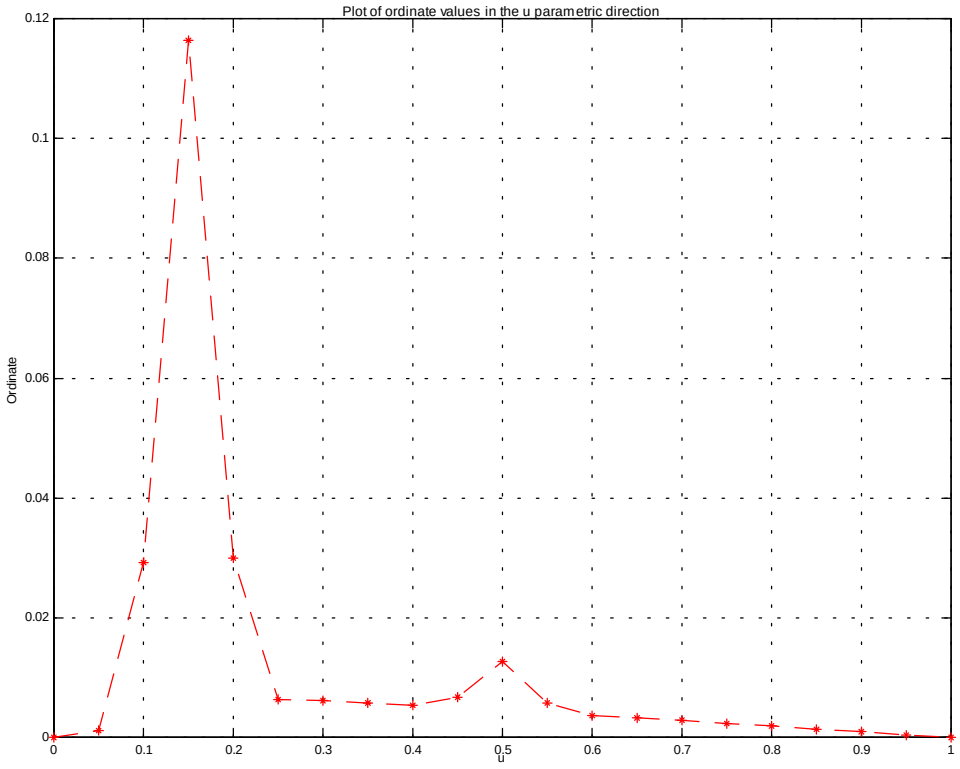

Figure 7.12: Case (ii) - Ordinate plot in the u direction replicating the shape of the error surface in that direction.

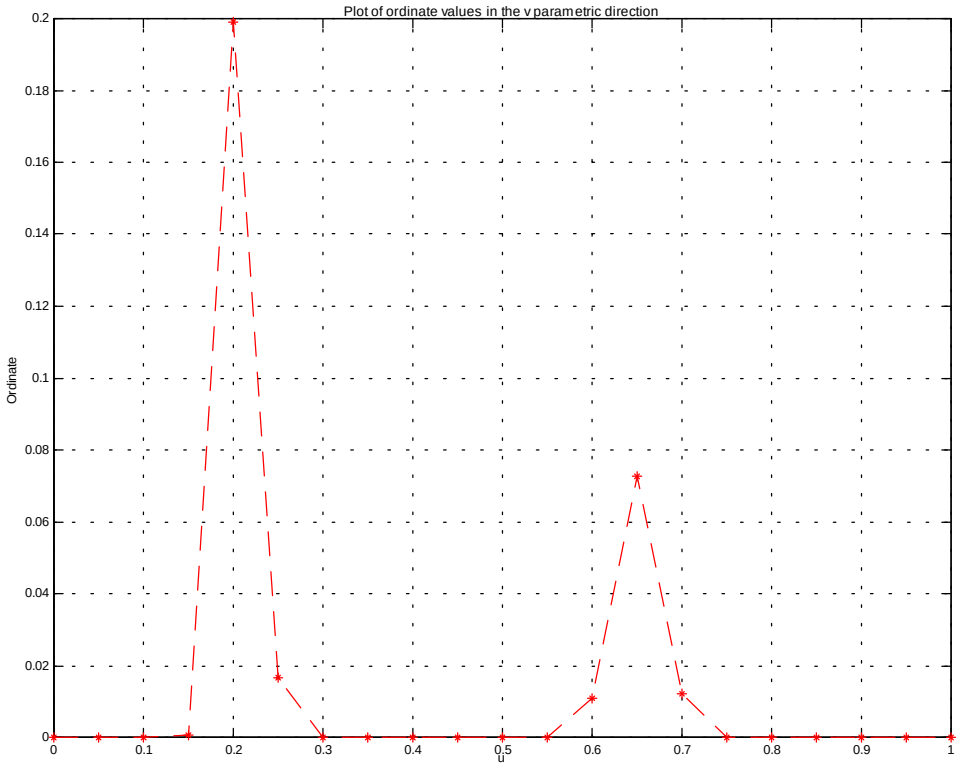

Figure 7.13: Case (ii) - Ordinate plot in the v direction replicating the shape of the error surface in that direction.

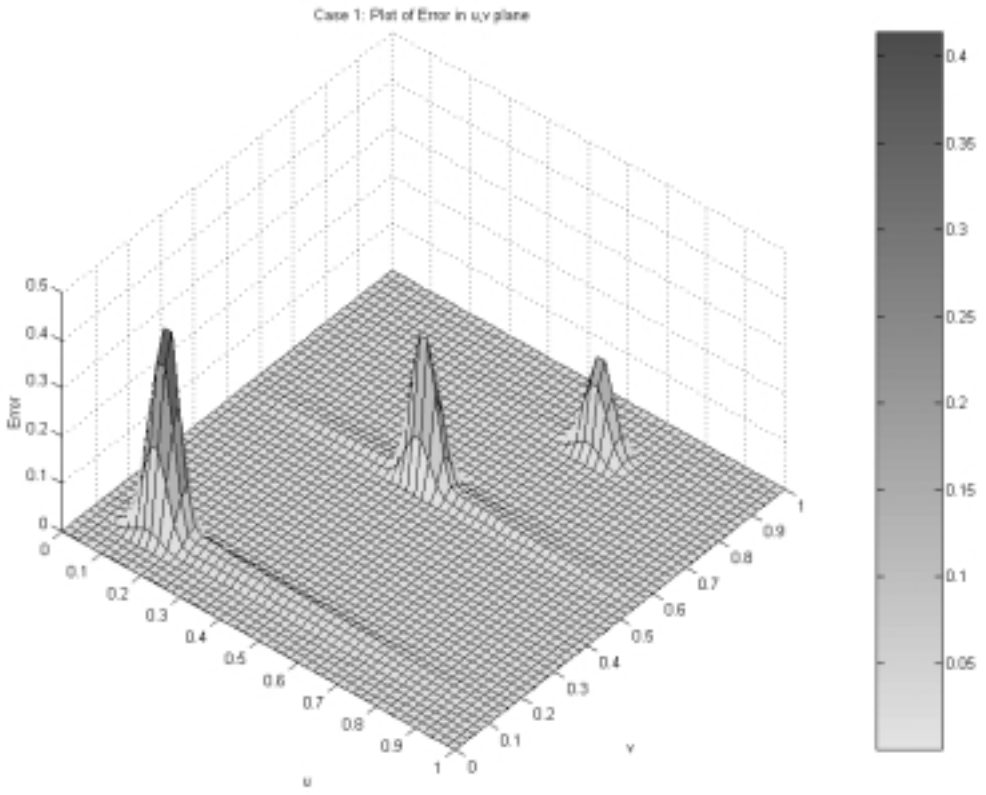

Figure 7.14: Case (iii) - Error surface with three areas of position discrepancy shown in parametric plane. The number of points sampled here is 51 along each direction to obtain better resolution.

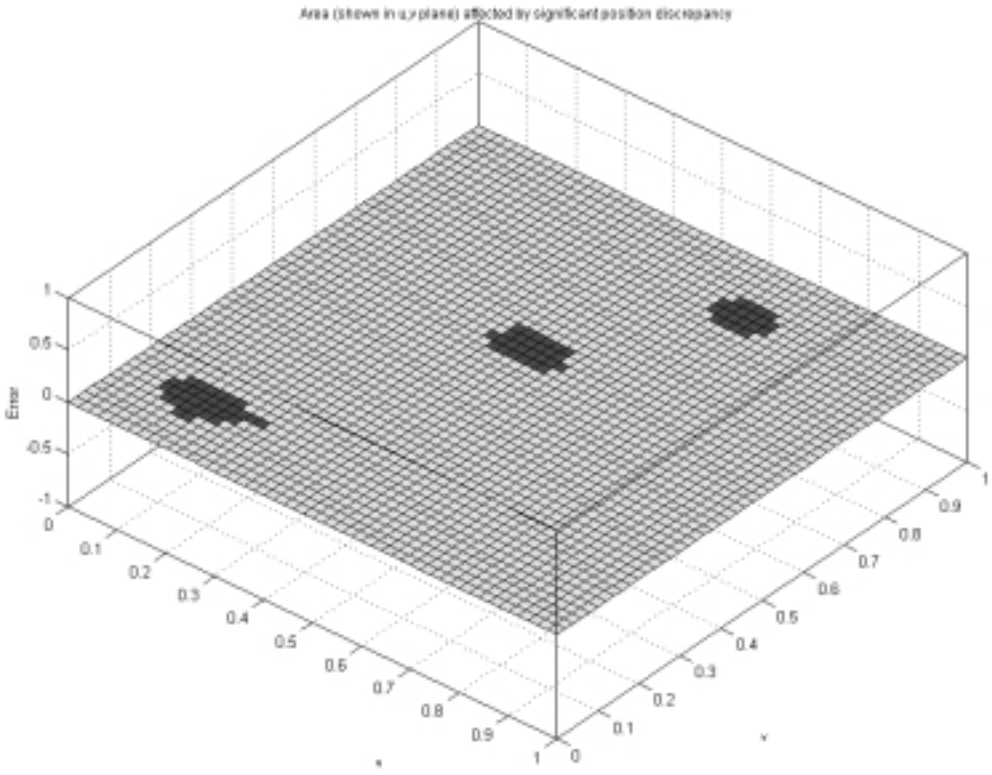

Figure 7.15: Case (iii) - Areas of significant position discrepancy shown on parametric plane. An increase in sampling rate improves the resolution of the dscrepancy on the plot.

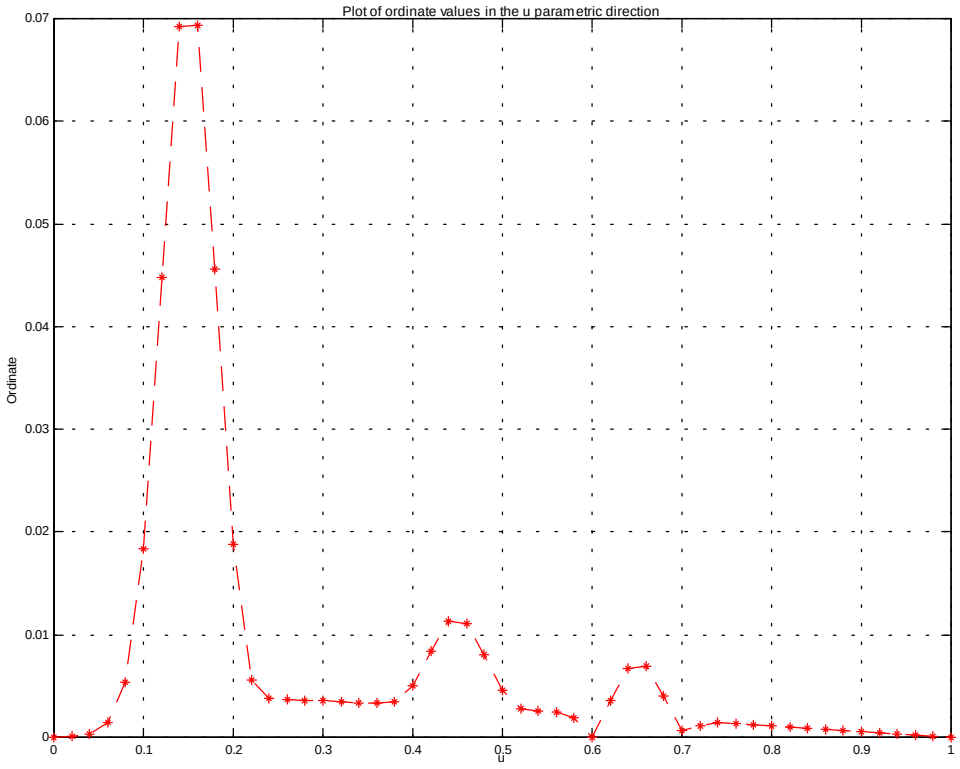

Figure 7.16: Case (iii) - Ordinate plot in the u direction replicating the shape of the error surface in that direction. Here again, the increased resolution is evident.

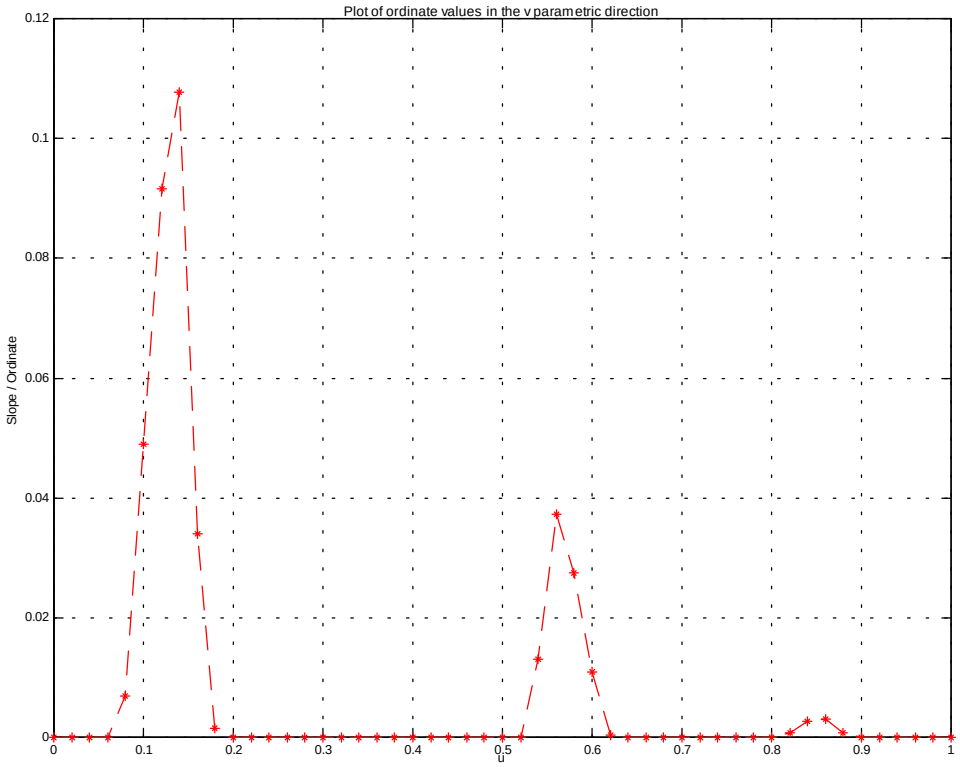

Figure 7.17: Case (iii) - Ordinate plot in the v direction replicating the shape of the error surface in that direction. The increase in number of points sampled improves the resolution.

The results presented till now have focussed on trapping position discrepancy between matching surfaces. In the following paragraphs, other methods will be discussed. It would be worthwhile to remember that most of these methods use the data reduction scheme discussed in the preceding paragraphs. The next paragraph presents results obtained from the Fourier analysis of the error plot.

The feasibility of Fourier analysis as an error visualization tool has been established in an earlier chapter on the same subject. The problem here also is essentially one of data reduction and subsequently of graphical presentation. In this research, data resulting from a discrete Fourier analysis has been abstracted in two stages. For the first stage, Fourier or harmonic coefficients are calculated for error values along an isoparametric curve and then the sum of the first six coefficients is plotted against the parameter value in the other parametric direction. Here, the number six is chosen empirically as higher harmonics for most closely matching surfaces were found to have a nearly insignificant contribution on the frequency spectrum. The focus is to avoid information overload for the designer and instead convey meaningful information only. Since the Fourier coefficients essentially describe or rather distribute the data among various frequency components, the frequency spectrum along a parametric direction closely models the shape of the error plot.

The second stage of abstraction is based on the assumption that; for a closely matched surface, the first harmonic will have a dominant role in the frequency spectrum of the error values. A comparison of the frequency spectra discussed later on in this section will

validate this assumption. However, in cases where higher harmonics are dominant, the surface match might not be a good one. This has already been demonstrated earlier by way of an exaggerated example. The reader will recall that three cases of localized error were discussed in the earlier section. This section discusses the results of the harmonic analysis applied to the above three cases. Figures 7.18 through 7.23 display the sum of the first six coefficients in both u and v direction respectively for cases (i), (ii), and (iii) respectively. Figures 7.24 through 7.29 show the first harmonic coefficient plotted against parameter value for the same cases.

The reader will observe that harmonic analysis is a tool that analyzes the quality of the match between two surfaces. As compared to the ordinate intercept plot, it might not be able to convey quantitative information about the position or magnitude of discrepancies, but it does convey important information about the match requiring just a glance at the frequency spectrum. The next section presents results of comparison of surface normal values between the two surfaces.

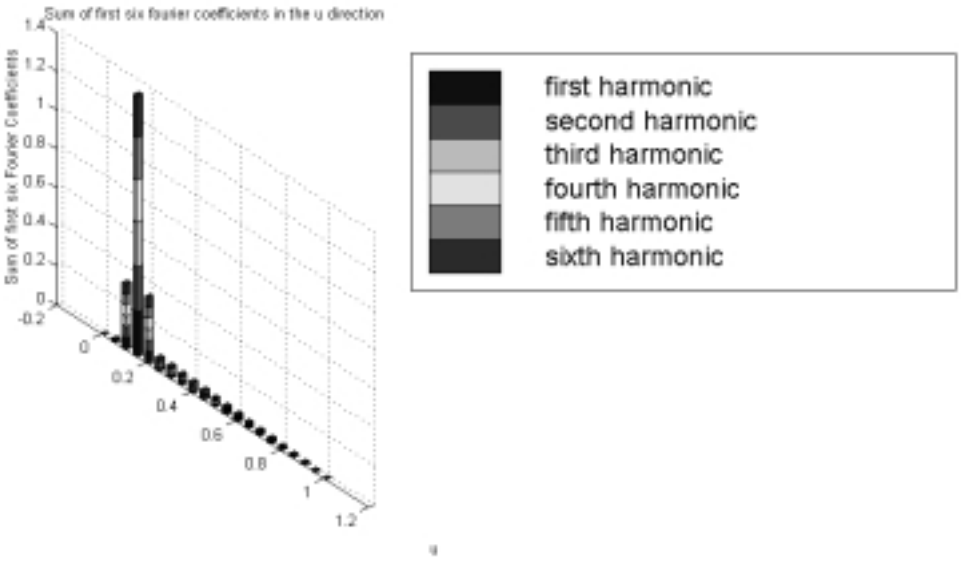

Figure 7.18: Case (i) - Sum of first six fourier coefficients against u parameter value plot. Fourier analysis is apllied to data collected along isoparametric curves in the u direction. The error surface for this analysis is shown in Figure 7.4.

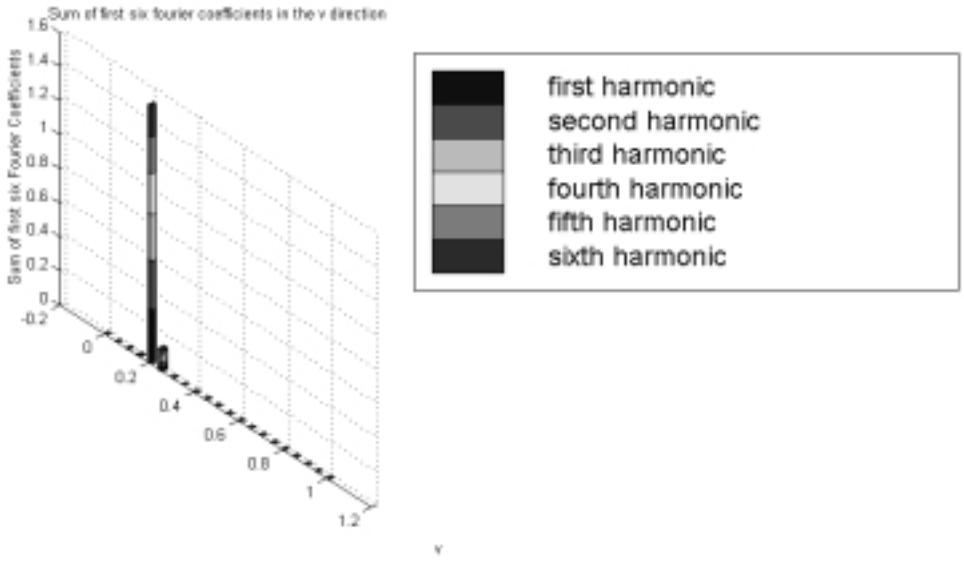

Figure 7.19: Case (i) - Sum of first six fourier coefficients against v parameter value plot. Fourier analysis is apllied to data collected along isoparametric curves in the v direction. The error surface for this analysis is shown in Figure 7.4.

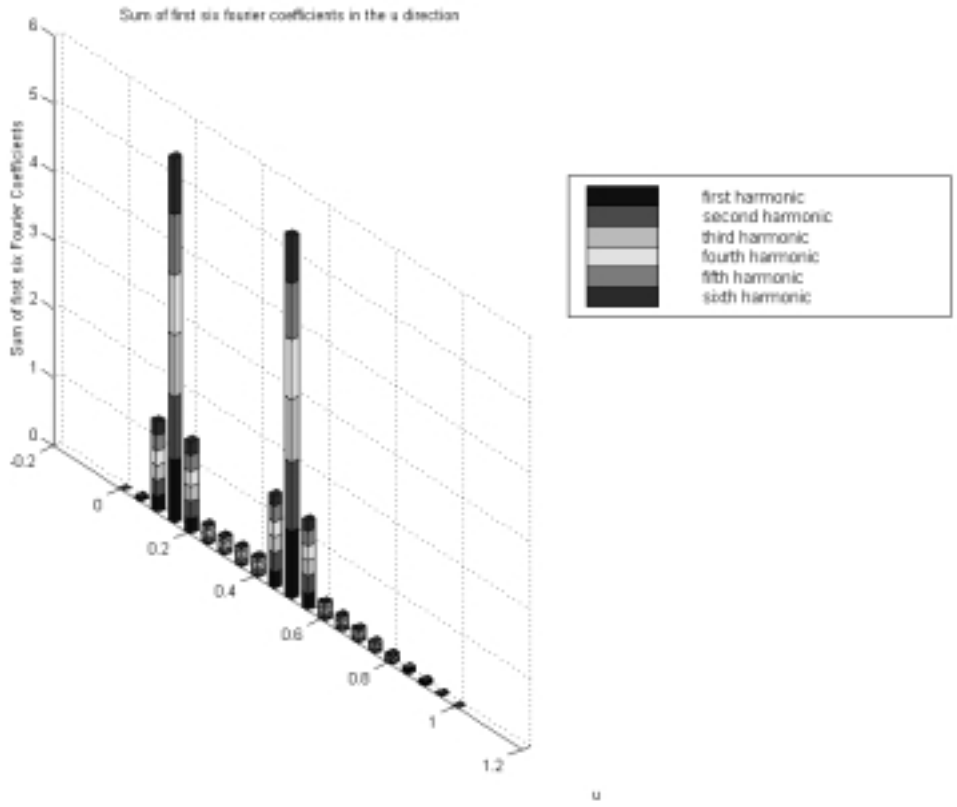

Figure 7.20: Case (ii) - Sum of first six fourier coefficients against u parameter value plot. Fourier analysis is applied to data collected along isoparametric curves in the u direction. The error surface for this analysis is shown in Figure 7.11.

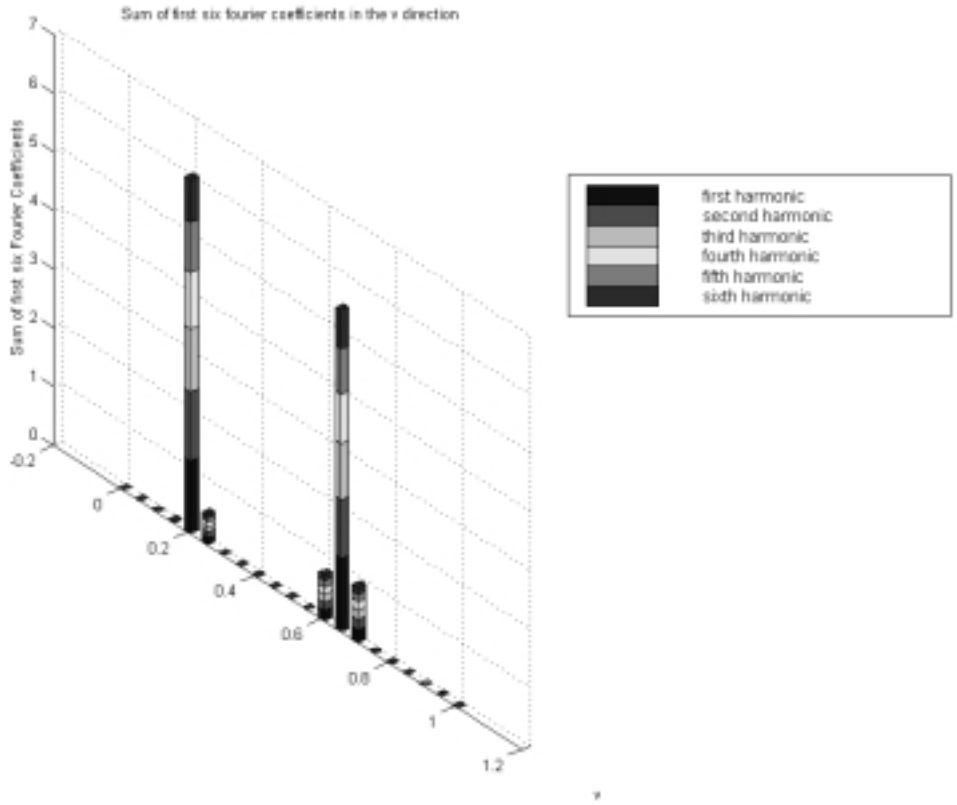

Figure 7.21: Case (ii) - Sum of first six fourier coefficients against v parameter value plot. Fourier analysis is applied to data collected along isoparametric curves in the v direction. The error surface for this analysis is shown in Figure 7.11.

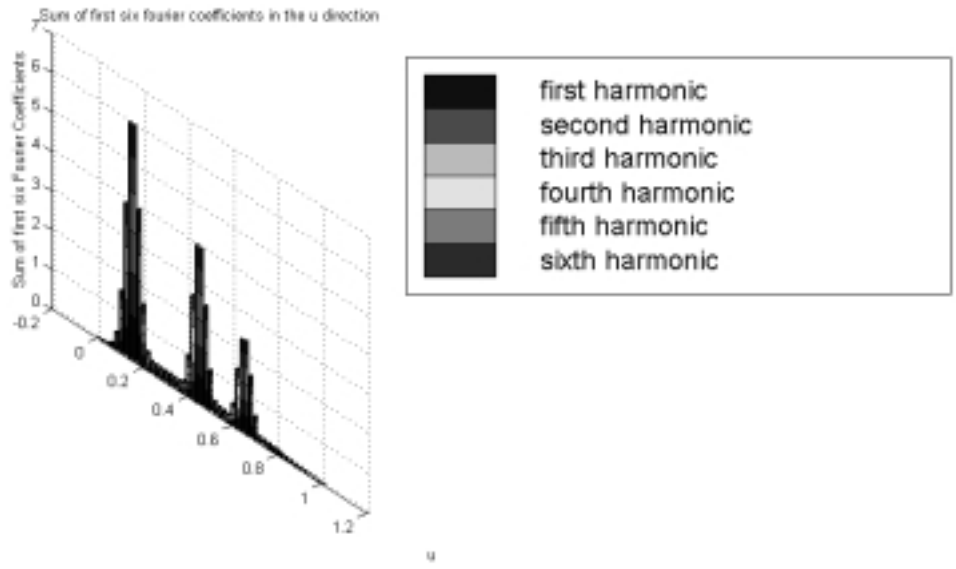

Figure 7.22: Case (iii) - Sum of first six fourier coefficients against u parameter value plot. Fourier analysis is applied to data collected along isoparametric curves in the u direction. The error surface for this analysis is shown in Figure 7.15. The increase in number of points sampled improves the resolution of the plot.

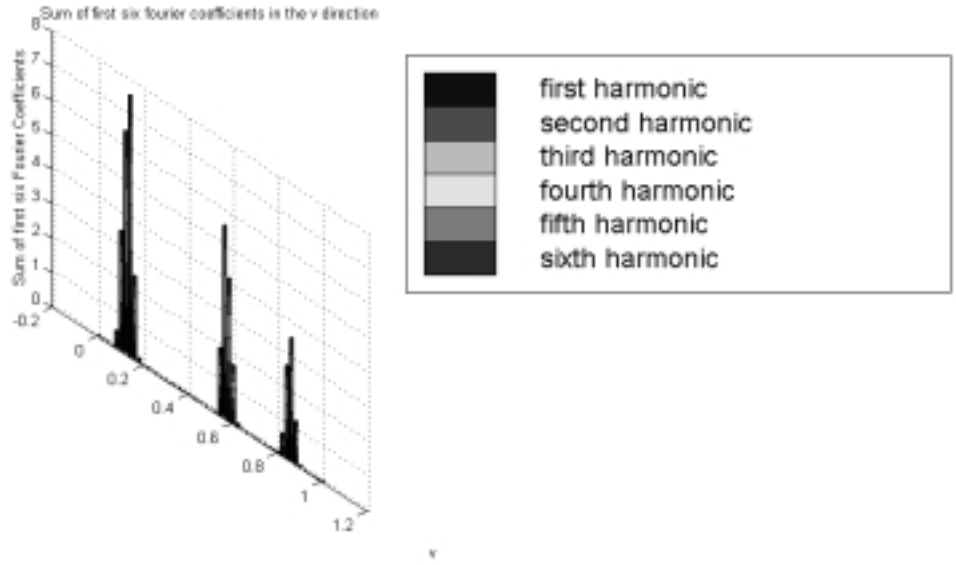

Figure 7.23: Case (iii) - Sum of first six fourier coefficients against v parameter value plot. Fourier analysis is applied to data collected along isoparametric curves in the v direction. The error surface for this analysis is shown in Figure 7.15. The increase in number of points sampled improves the resolution of the plot.

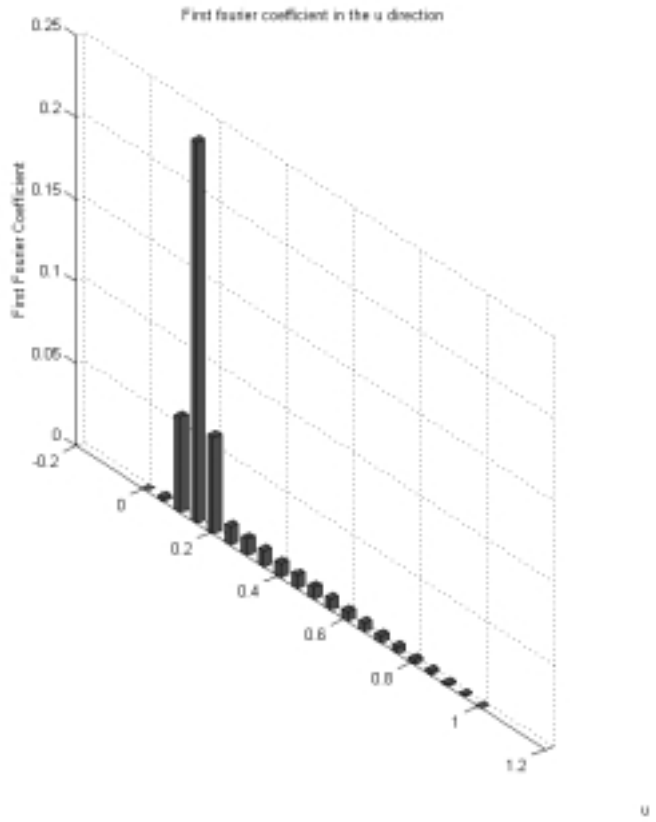

Figure 7.24: Case (i) - First harmonic coefficient along u parametric direction plotted against the parameter in the other direction for a surface with one defect. The corresponding error surface is shown in Figure 7.4 and the corresponding sum of six fourier plot is given in Figure 7.18.

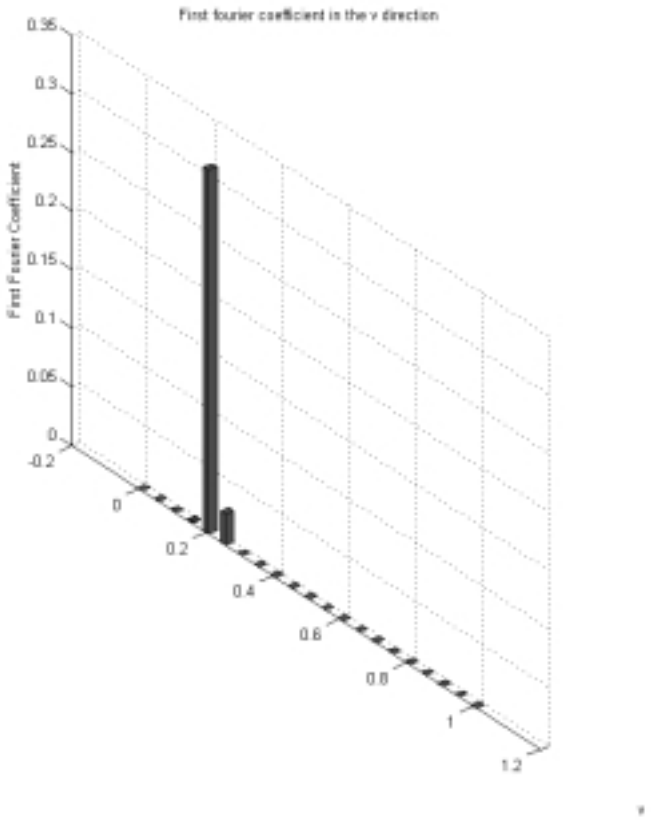

Figure 7.25: Case (i) - First harmonic coefficient along v parametric direction plotted against the parameter in the other direction for a surface with one defect. The corresponding error surface is shown in Figure 7.4 and the corresponding sum of six fourier plot is given in Figure 7.19.

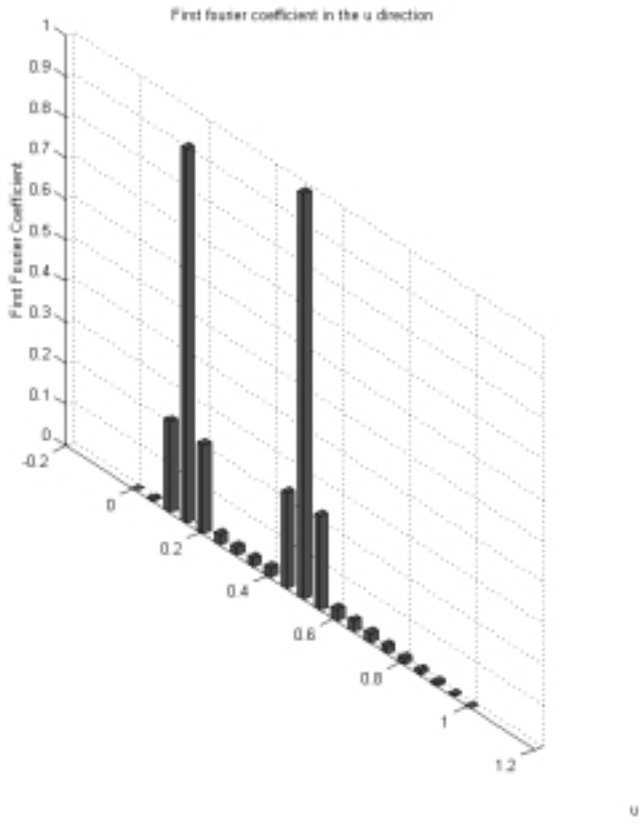

Figure 7.26: Case (ii) - First harmonic coefficient along u parametric direction plotted against the parameter in the other direction for a surface with two defects. The corresponding error surface is shown in Figure 7.10 and the corresponding sum of six fourier plot is given in Figure 7.20.

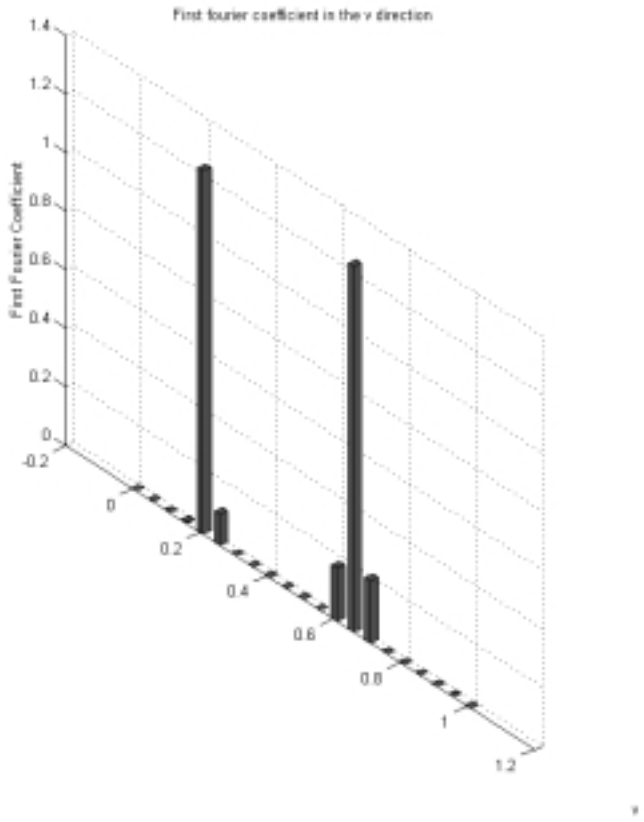

Figure 7.27: Case (ii) - First harmonic coefficient along v parametric direction plotted against the parameter in the other direction for a surface with two defects. The corresponding error surface is shown in Figure 7.10 and the corresponding sum of six fourier plot is given in Figure 7.20.

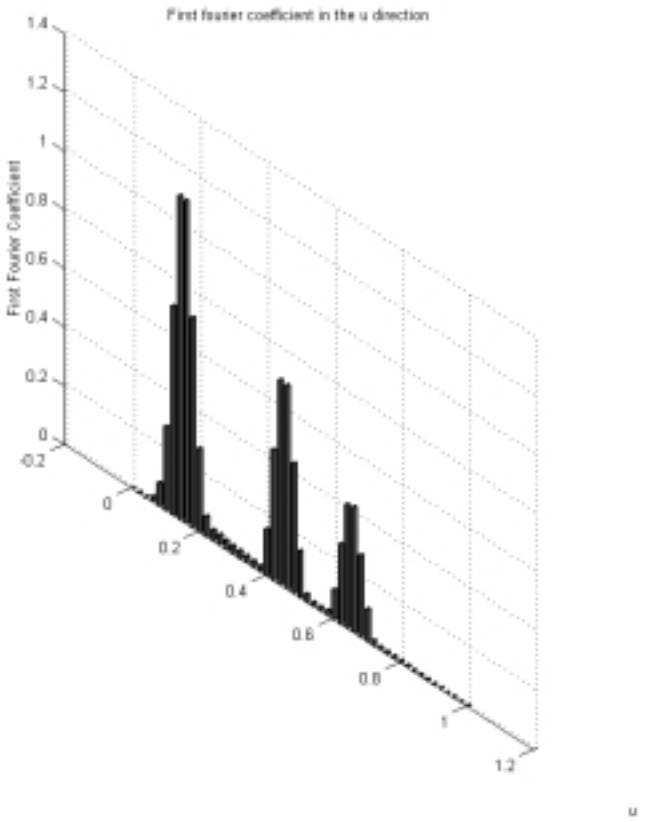

Figure 7.28: Case (iii) - First harmonic coefficient along u parametric direction plotted against the parameter in the other direction for a surface with three defects. The corresponding error surface is shown in Figure 7.14 and the corresponding sum of six fourier plot is given in Figure 7.21. Note the increase in resolution due to an increase in the number of points sampled.

Another tool that has been implemented in this research is the calculation of surface

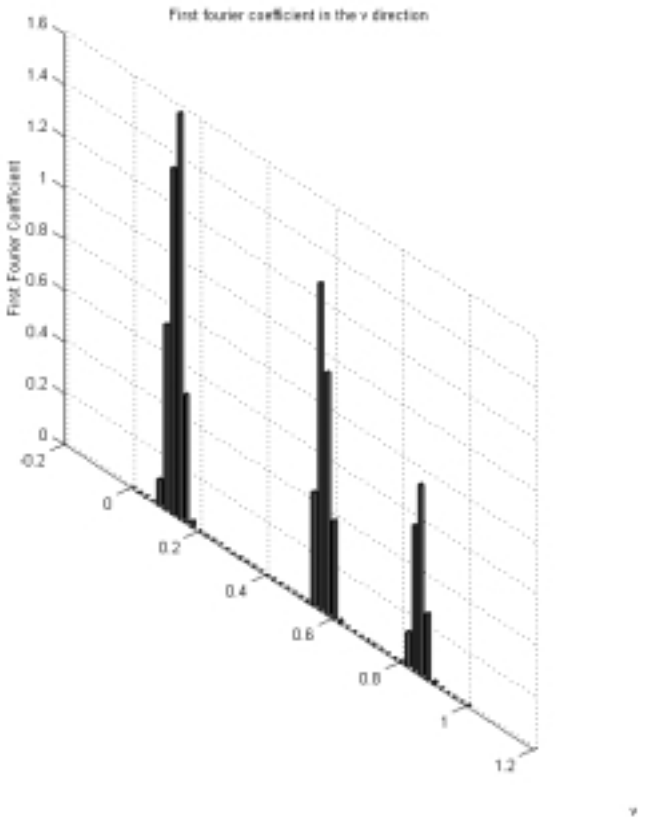

Figure 7.29: Case (iii) - First harmonic coefficient along v parametric direction plotted against the parameter in the other direction for a surface with three defects. The corresponding error surface is shown in Figure 7.14 and the corresponding sum of six fourier plot is given in Figure 7.22. Note the increase in resolution due to an increase in the number of points sampled.

normals on the original and the matching surface. If the two surfaces are perfectly matched, then the normals on the two will coincide. However, in a practical situation, this will never be the case. Therefore the comparison of surface normals data at various points constitutes a valuable error visualization tool. The reduction and presentation of data is done using the same scheme as for the position error visualization. However, in

this case, the angle between surface normals is used instead of the distance. Case (iv) discusses the comparison of surface normals for two patches that are identical except for a small area of localized error. Figures 7.30 through 7.33 show the position error plot, angle error plot, and the ordinate plot for angular separation resulting from linear fit. However, the surface normals plot can give the reader additional information when the matching surface has a twist or bend that drastically increases the angle between the surface normals. Case (v) presents the results for two such surfaces. Figure 7.34 through 7.37 illustrate the position error plot, the angle plot, as well as the ordinate plots in both directions. The reader can discern that one of the glitches has a pronounced twist in the orientation of the matching surface. In fact, the ordinate plot of the angle between surface normals in the u direction clearly shows that the angle difference between surface normals is quite pronounced for one of the glitches as compared to the other one. Although, the mathematical tools needed for calculating the surface normals have been discussed in an earlier section, the data used here is directly obtained from I-DEAS.

Table 7.5: Case (iv) – Table showing the comparison between correlation values obtained from angle

Results along u parametric direction	
Correlation coefficient between 21 maximum values of angle error and ordinate intercept values	0.792817
Correlation coefficient between 21 maximum values of position error and ordinate intercept values	0.972614
Results along v parametric direction	
Correlation coefficient between 21 maximum values of angle error and ordinate intercept values	0.704119
Correlation coefficient between 21 maximum values of angle error and ordinate intercept values	0.99923

Table 7.6: Case (v) – Table showing the comparison between correlation values obtained from angle error plot and the ones obtained from position error plot.

Results along u parametric direction	
Correlation coefficient between 21 maximum values of angle error and ordinate intercept values	0.998530
Correlation coefficient between 21 maximum values of position error and ordinate intercept values	0.977089
Results along v parametric direction	
Correlation coefficient between 21 maximum values of angle error and ordinate intercept values	0.952722
Correlation coefficient between 21 maximum values of angle error and ordinate intercept values	0.972593

Tables 7.5 and 7.6 respectively compare the results of correlation between ordinate intercept values and the maximum values of angle error to the correlation between ordinate intercept values with the maximum values of position error for cases (iv) and (v). There are a couple of points worth noting with respect to the calculations that yield surface normals. Firstly, the two surface descriptions (for the original and the matching surface) are different and as such points at which normals are calculated are equivalent only in the parametric domain. Secondly, it is possible that the orientation of the surface normals at a point that has significant position error is either same or comparable. The designer always has to keep this possibility in mind while interpreting results obtained from comparison of surface normals. However, as mentioned earlier, this method has tremendous value as it gives the designer information about the relative orientation of the points on isoparametric curves on the two surfaces. The next section discusses the use of curvature values on isoparametric as measure of error between two matching surfaces.

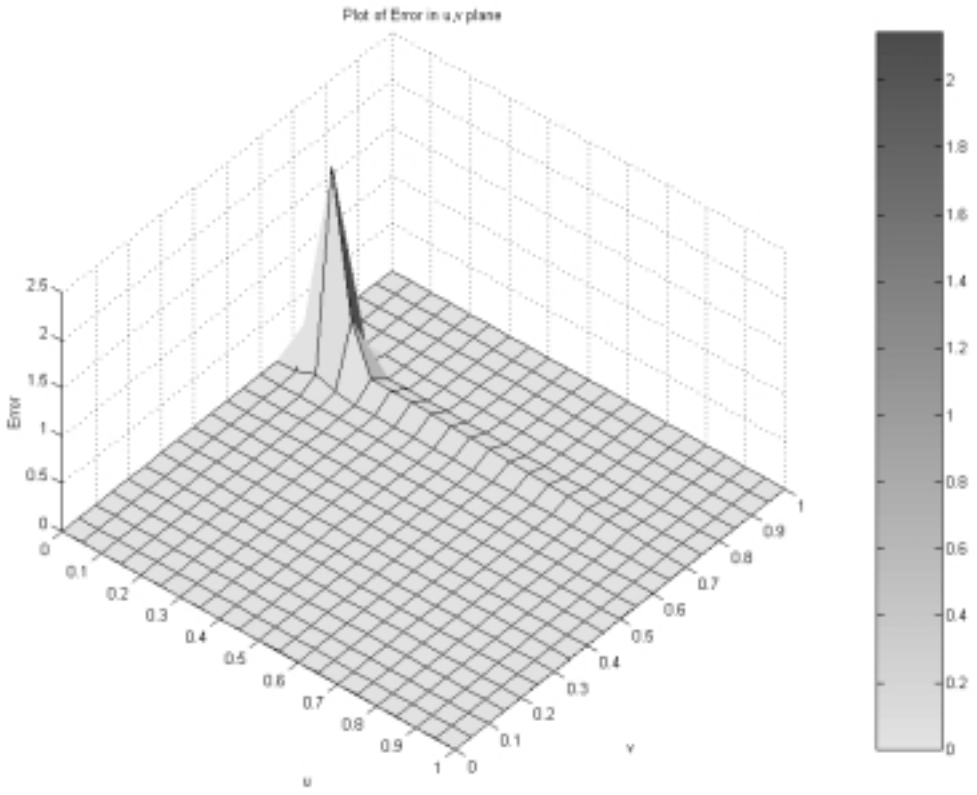

Figure 7.30: Case (iv) - Error surface for a matching surface with one deformity shown in parametric plane for comparing with information provided by the angle between surface normals plot. The bar on the left color codes the distances on the plot.

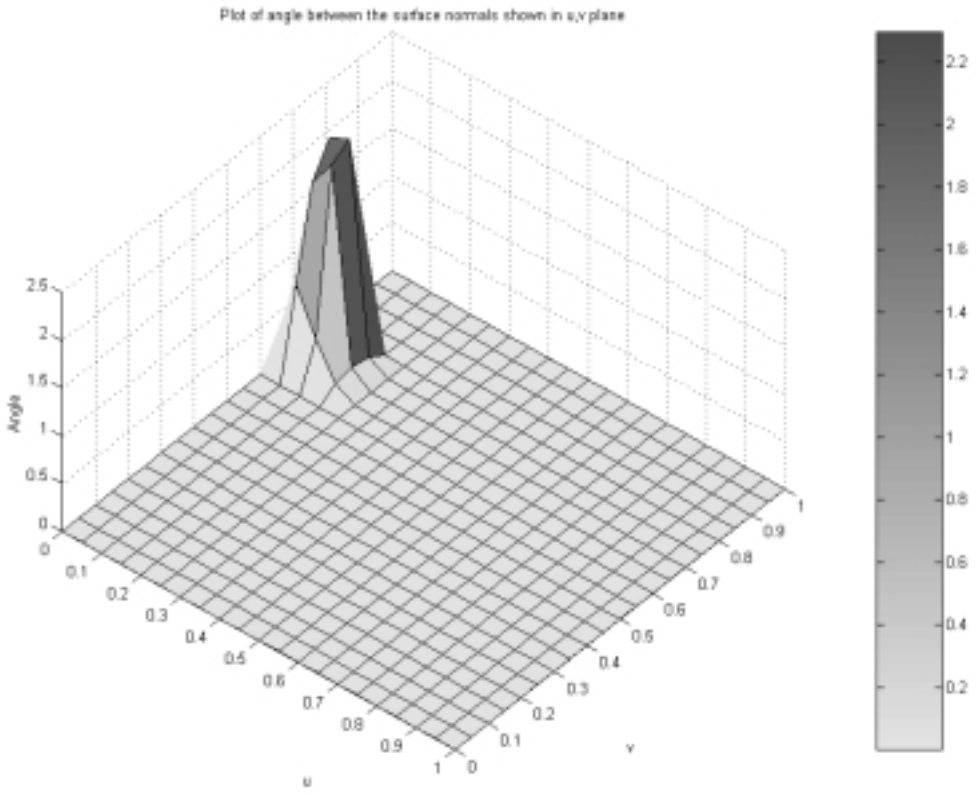

Figure 7.31: Case (iv) - Plot showing the angle between surface normals for the original and the matching surface. The Figure (7.31) shows the error surface that corresponds to this plot.

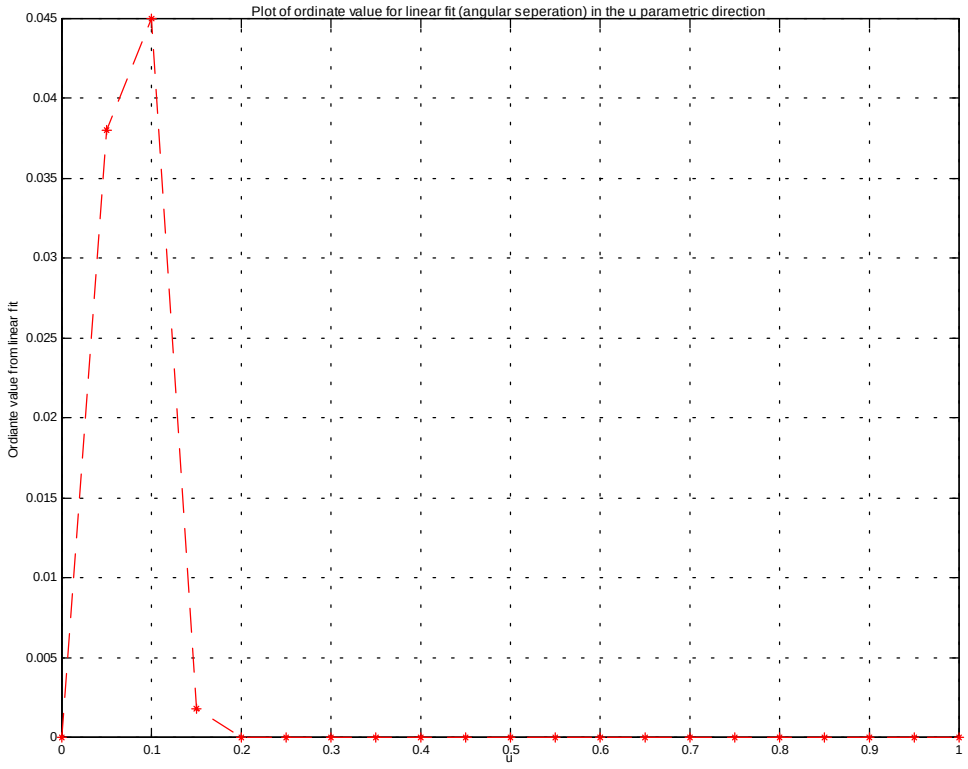

Figure 7.32: Case (iv) - Ordinate plot in the u parametric direction obtained from fitting linear elements to the angle between surface normals. The data reduction scheme followed is same as the position error data reduction scheme

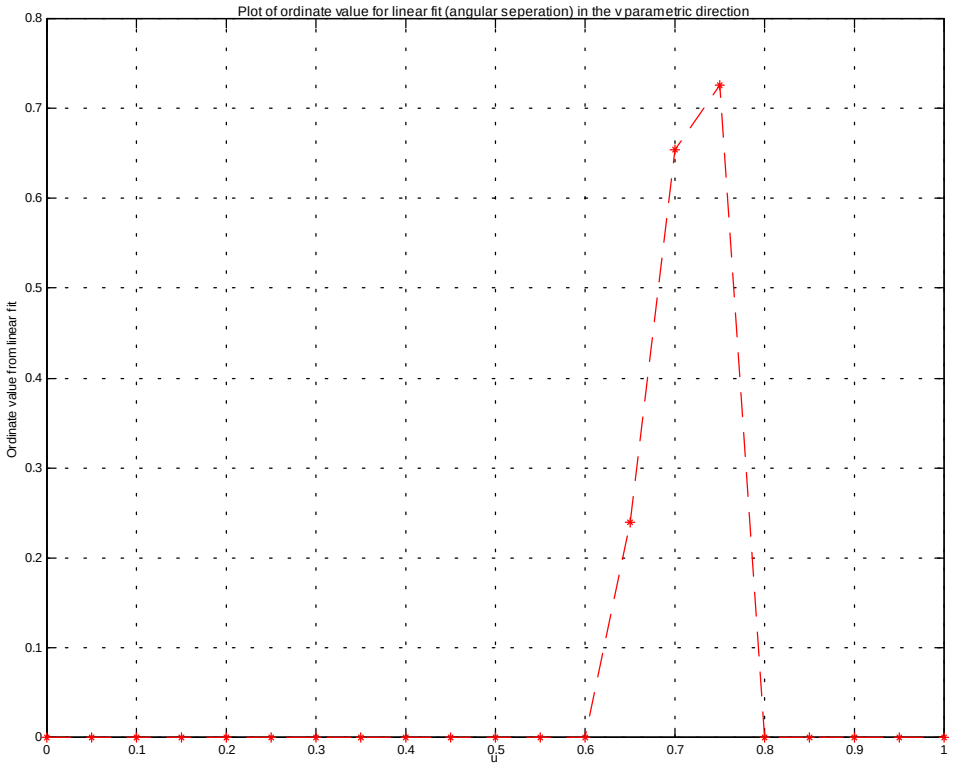

Figure 7.33: Case (iv) - Ordinate plot in the v parametric direction obtained from fitting linear elements to the angle between surface normals. The data reduction scheme followed is same as the position error data reduction scheme

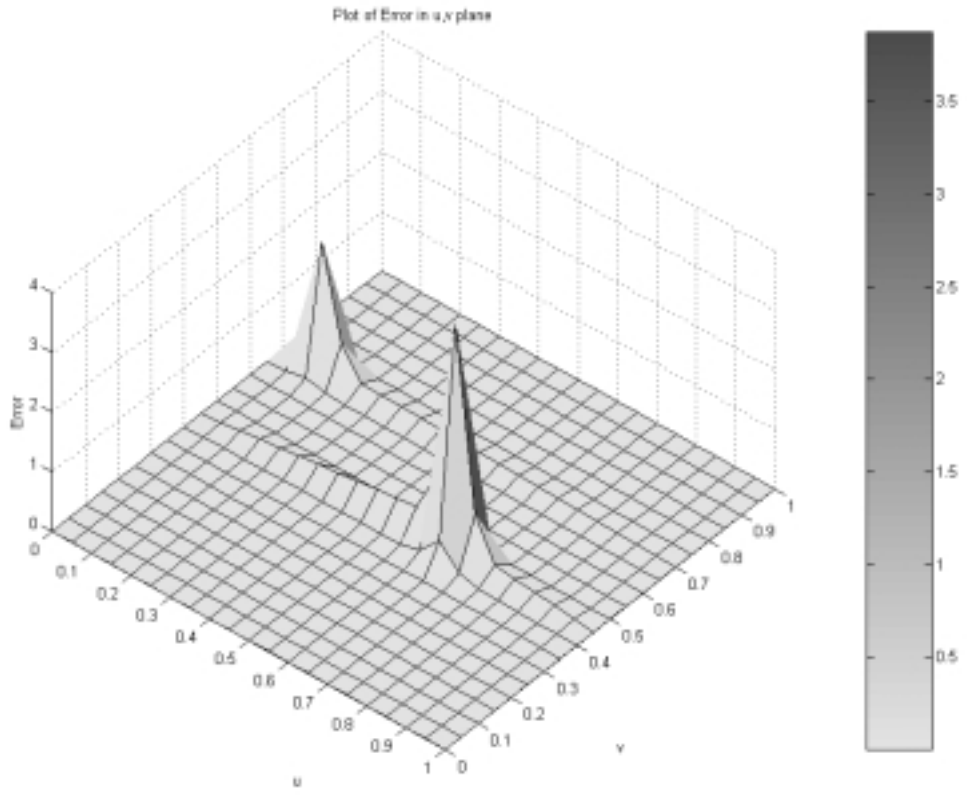

Figure 7.34: Case (v) - Error surface for a case where the matching surface has two glitches. The error surface is shown to contrast information that may be discerned from a plot of surface normals.

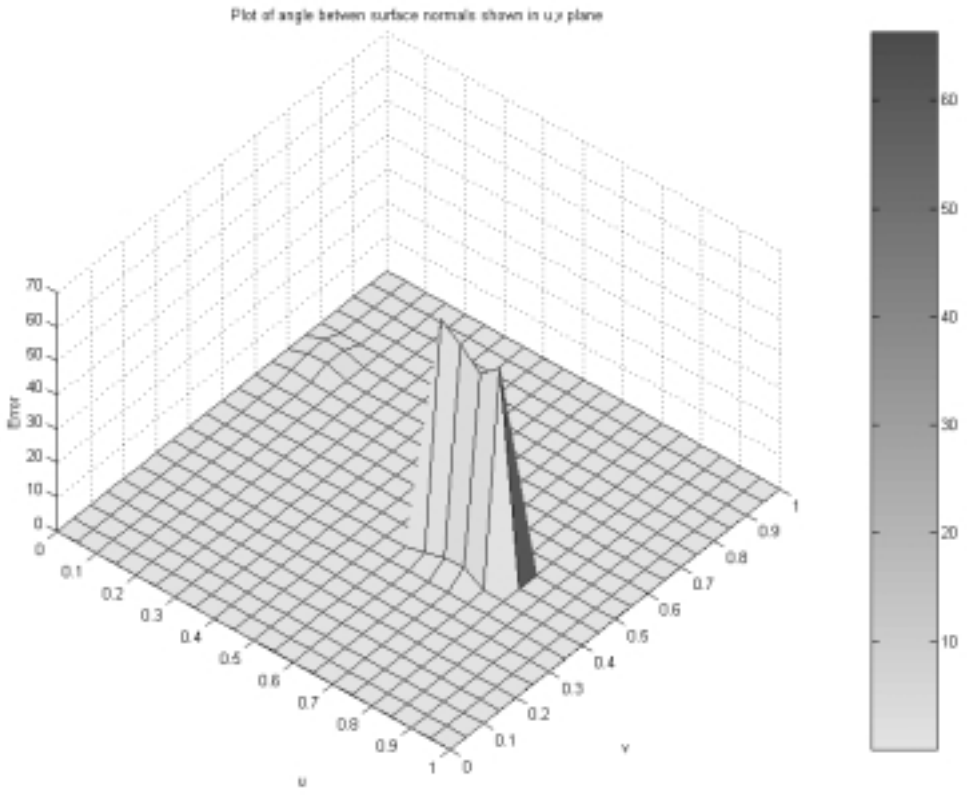

Figure 7.35: Case (v) - Plot of angle between surface normals for the error surface of figure (7.34). The difference between angle magnitudes for the two glitches clearly suggests that one of them has a pronounced twist in its orientation in 3-D space.

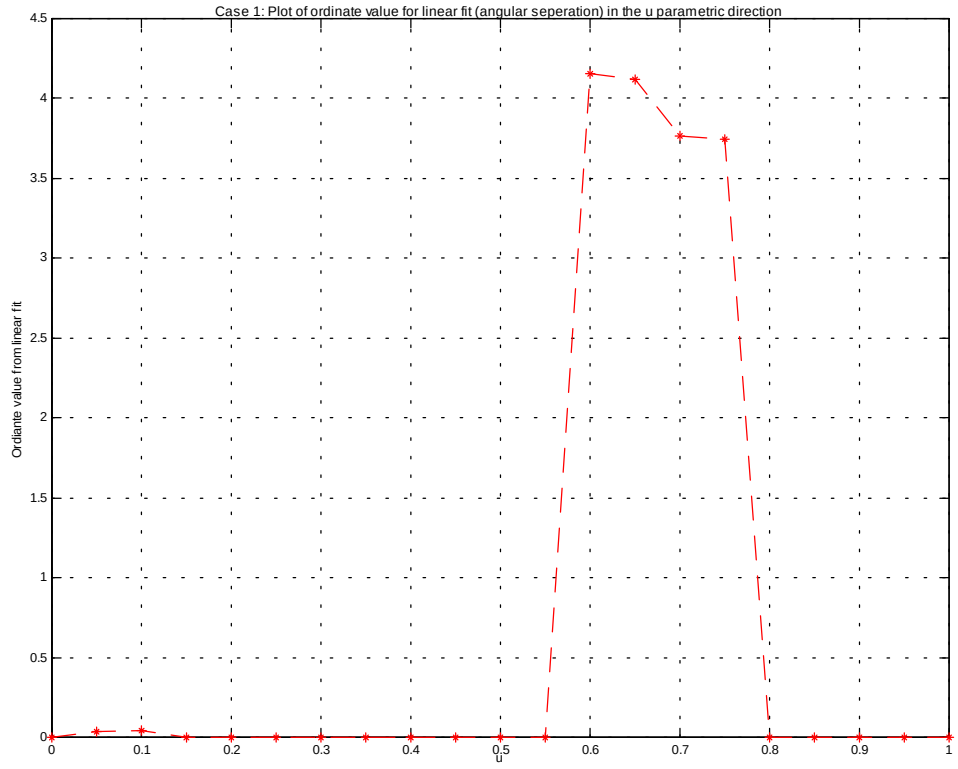

Figure 7.36: Case (v) - Ordinate plot showing linear fit values along isoparametric lines in the u parametric direction. This condensation accurately conveys the difference in orientation between the two surfaces.

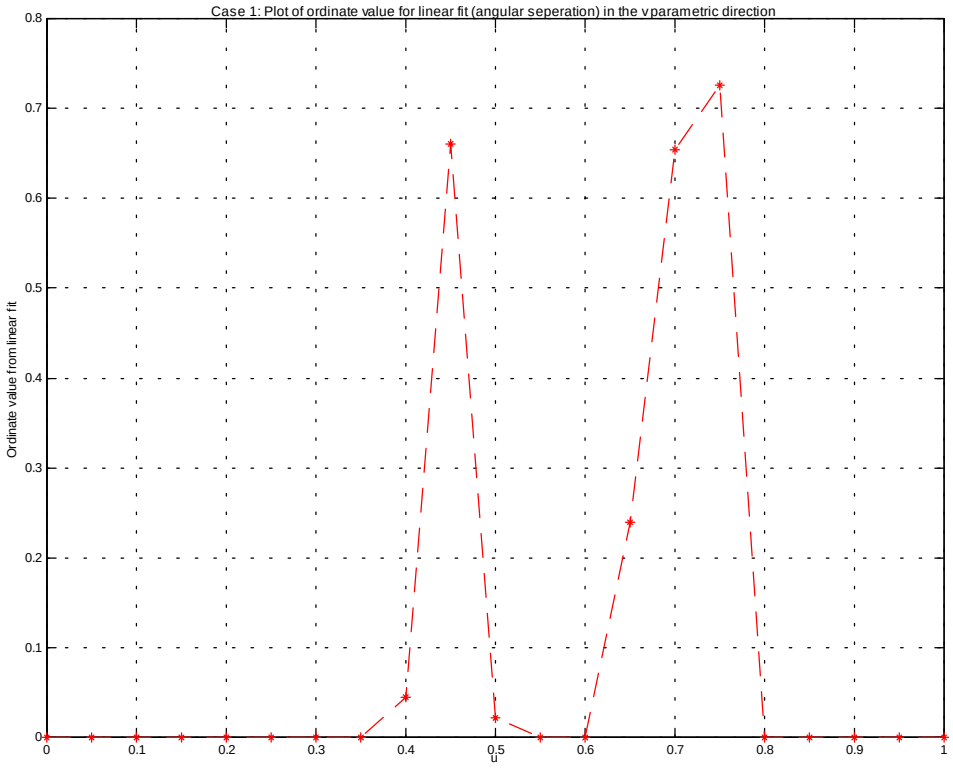

Figure 7.37: Case (v) - Ordinate plot showing linear fit values along isoparametric lines in the v parametric direction. This condensation does not accurately convey the difference in orientation as the plot in the u direction.

Comparing of radii of curvature values of corresponding points on the two surfaces also is a valuable tool for studying the behavior of a matching surface vis-à-vis the original. The radii of curvature values are calculated along isoparametric curves on each of the surfaces using mathematical tools discussed earlier. The data is reduced in a similar fashion to the position error data. Case (vi) discusses the results obtained from comparing the curvature values for two surfaces with one area of discrepancy. Figures (7.39) through (7.44) show the position error, difference in radii of curvature, and the ordinate intercept plots in either directions (radius of curvature condensation) for this case. Case (vii) discusses the results from comparison of two matching surfaces with two areas of discrepancy. Figures (7.45) through (7.50) show the position error, difference in radii of curvature, and the ordinate intercept plots in either direction (radius of curvature condensation).

The reader will observe from figures (7.39) and (7.45) that there is some noise present in the ordinate intercept plot of difference in radii of curvature values. Due to the presence of this extraneous noise, any calculation of correlation between the difference in radii of curvature for the two surfaces and the maximum error values is not very reliable. It should be pointed out that the ordinate intercept plot does indicate the major areas of defect between the two surfaces and as such, validates the results obtained by the ordinate intercept plot of the position differences. The difference in radius of curvature values would be zero or minimal for points along isoparametric curves on matching surfaces.

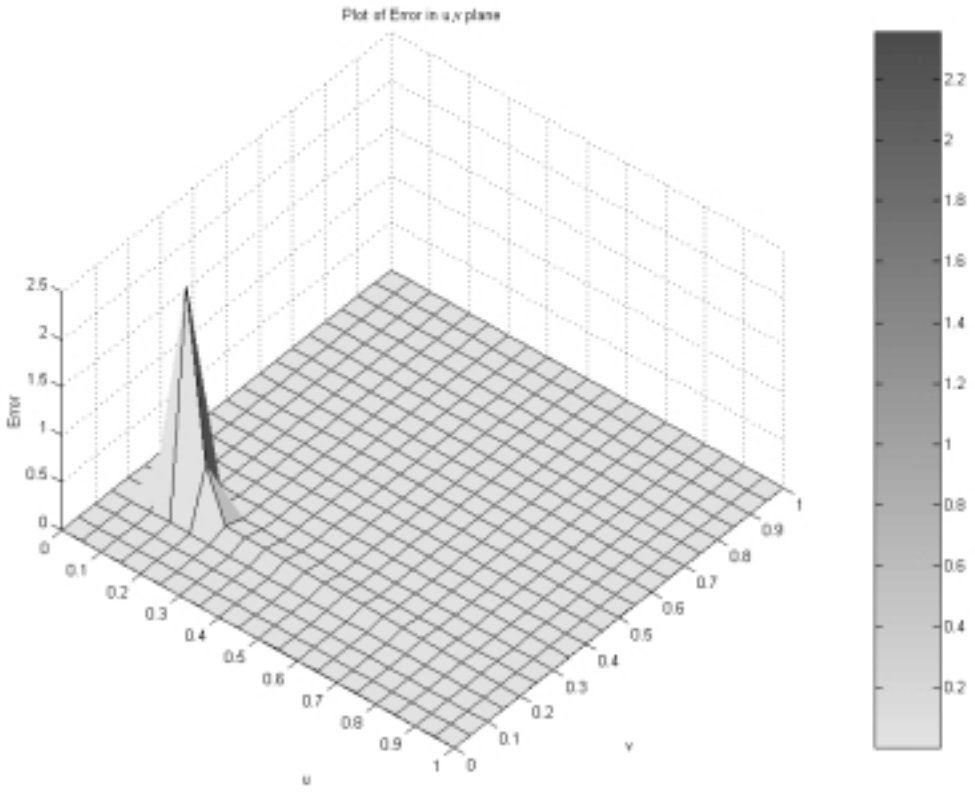

Figure 7.38: Case (vi) - Error plot for demonstrating that radius of curvature is a measure of the difference between two surfaces.

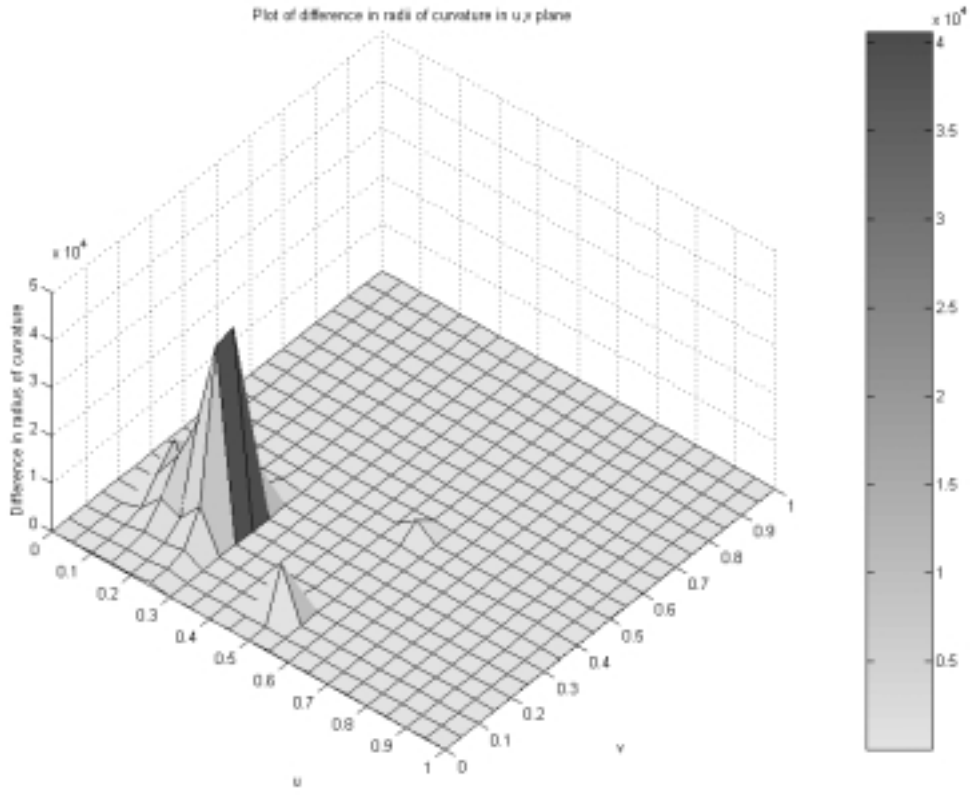

Figure 7.39: Case (vi) - Plot of difference in radii of curvature values for the error surface shown in figure (7.38). The data has some noise but does mimic the behavior of the prominent discrepancy.

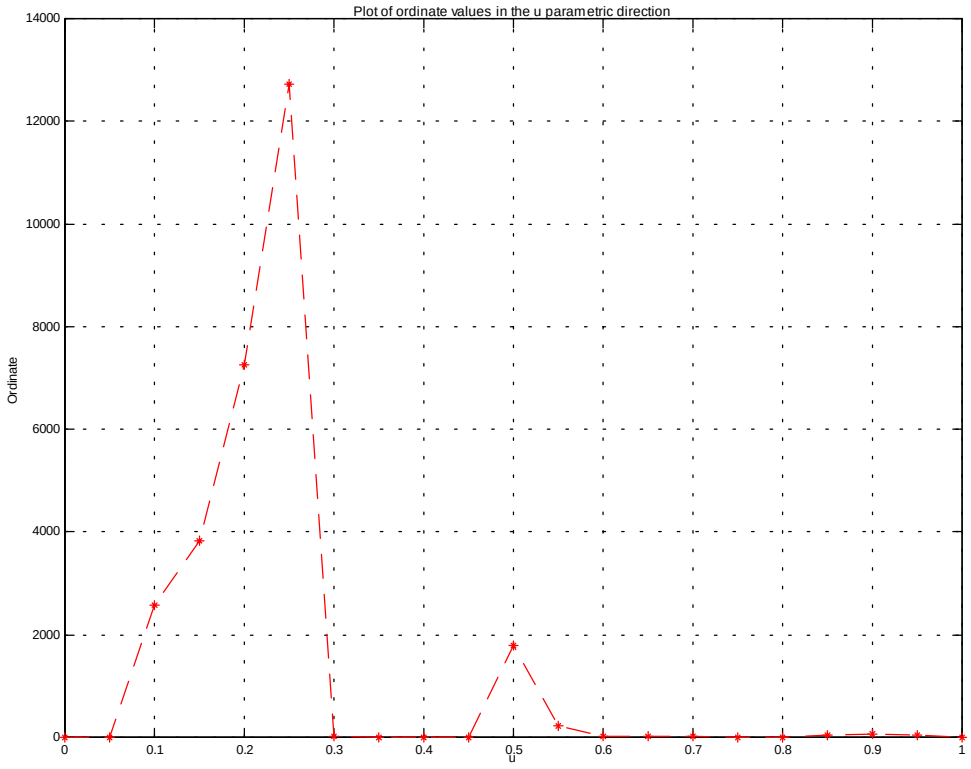

Figure 7.40: Case (vi) - Ordinate plot in u direction for fit of difference in radii of curvature values for the two surfaces.

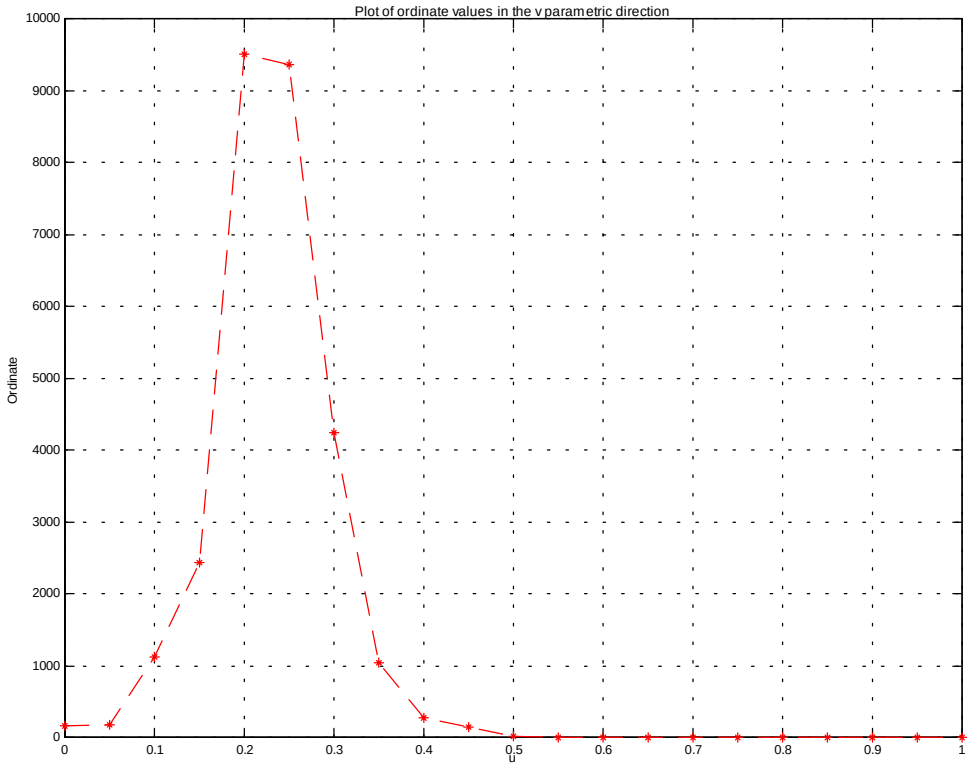

Figure 7.41: Case (vi) - Ordinate plot in v direction of difference in radii of curvature values for the error surface shown in figure (7.38).

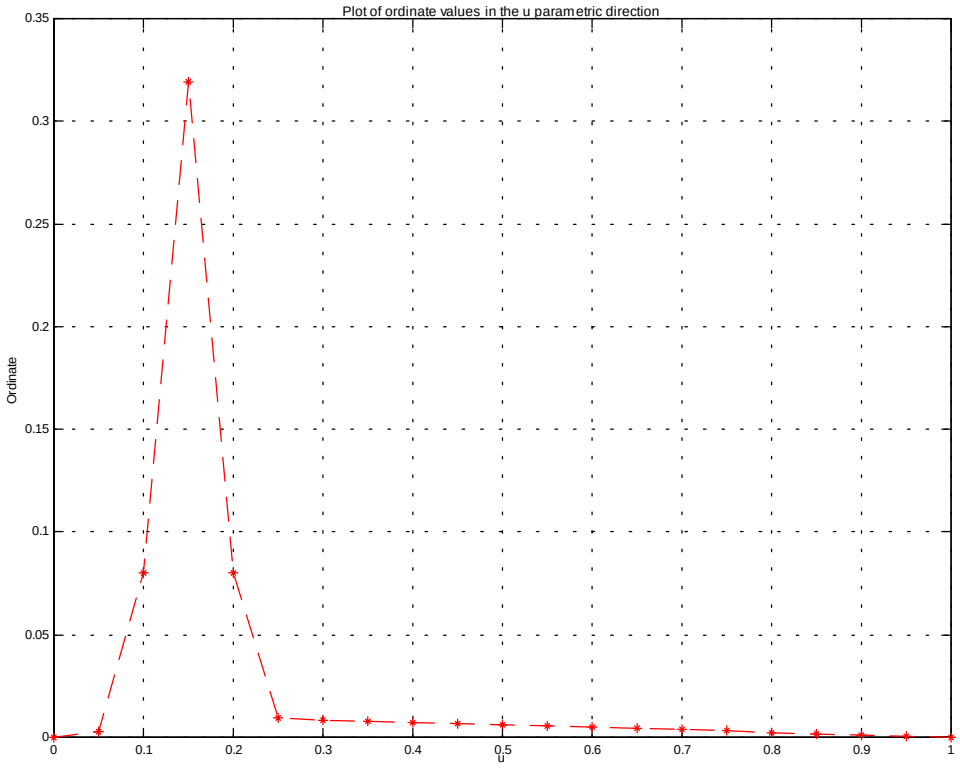

Figure 7.42: Case (vi) - Ordinate plot in u direction for the error surface shown in figure (7.38). This is included to compare the information garnered from the difference in radii of curvature values.

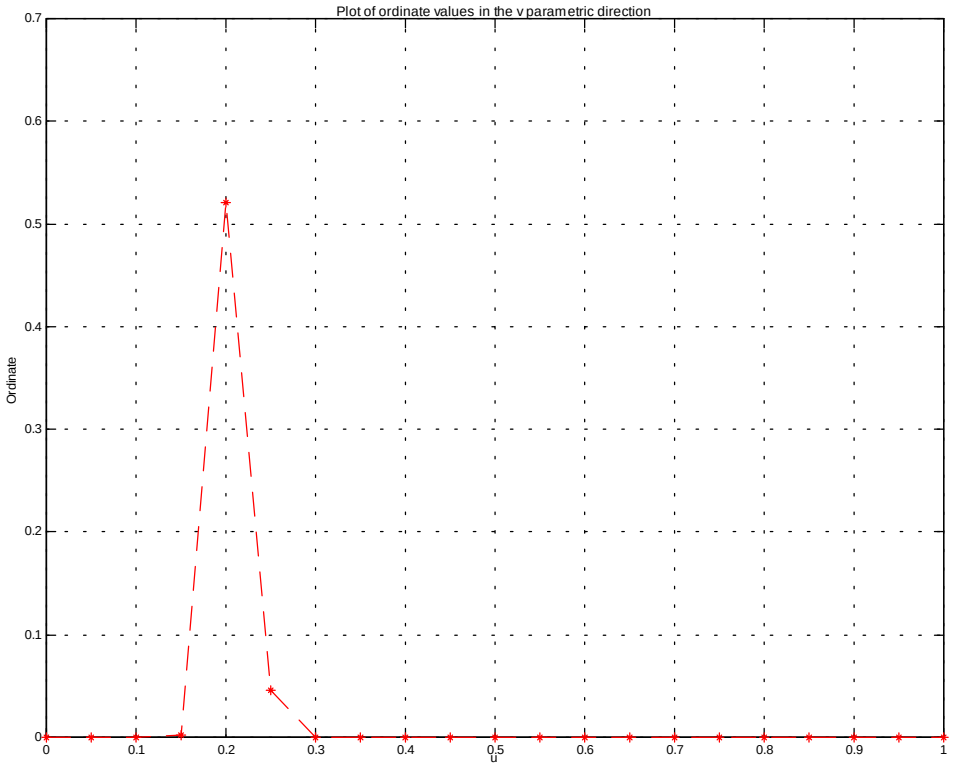

Figure 7.43: Case (vi) - Ordinate plot in u direction for the error surface shown in figure (7.38). This is included to compare the information garnered from the difference in radii of curvature values.

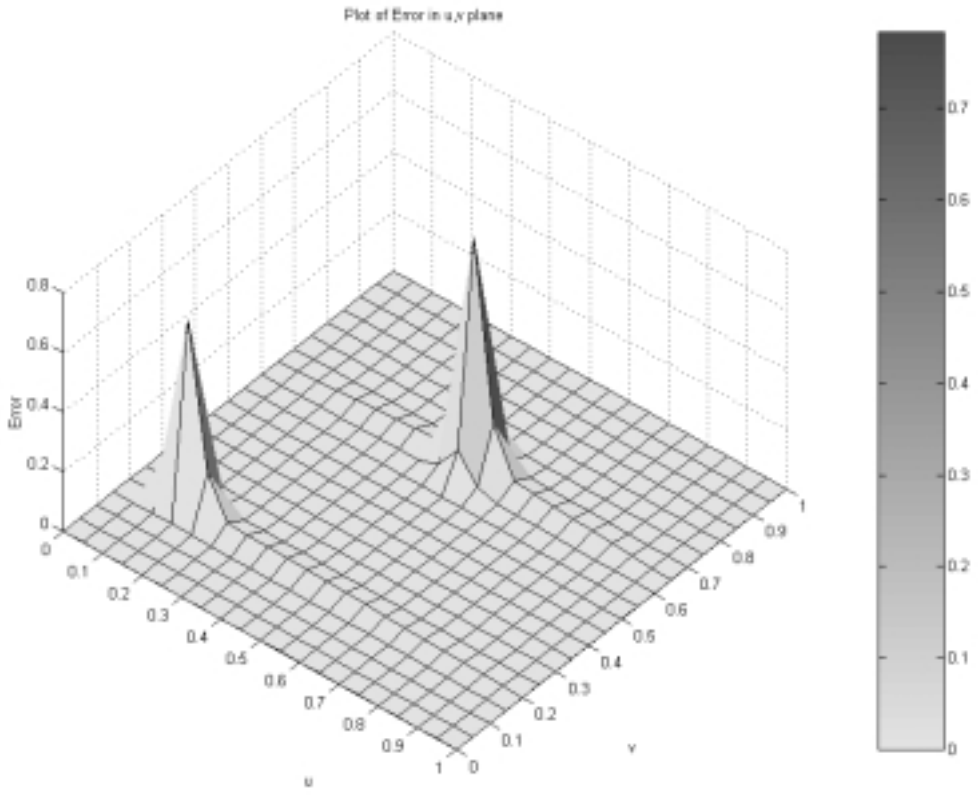

Figure 7.44: Case (vii) - Error surface shown in parametric plane with two discrepancies in position.

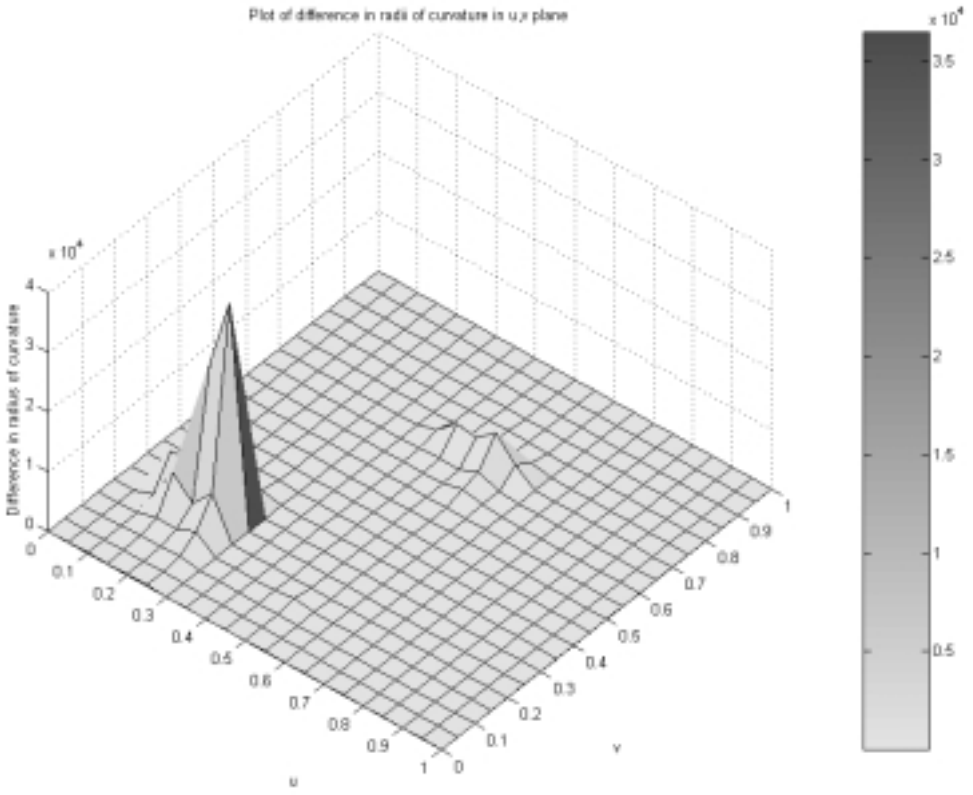

Figure 7.45: Case (vii) - Plot of difference in curvature values for the error surface shown in figure (7.44).

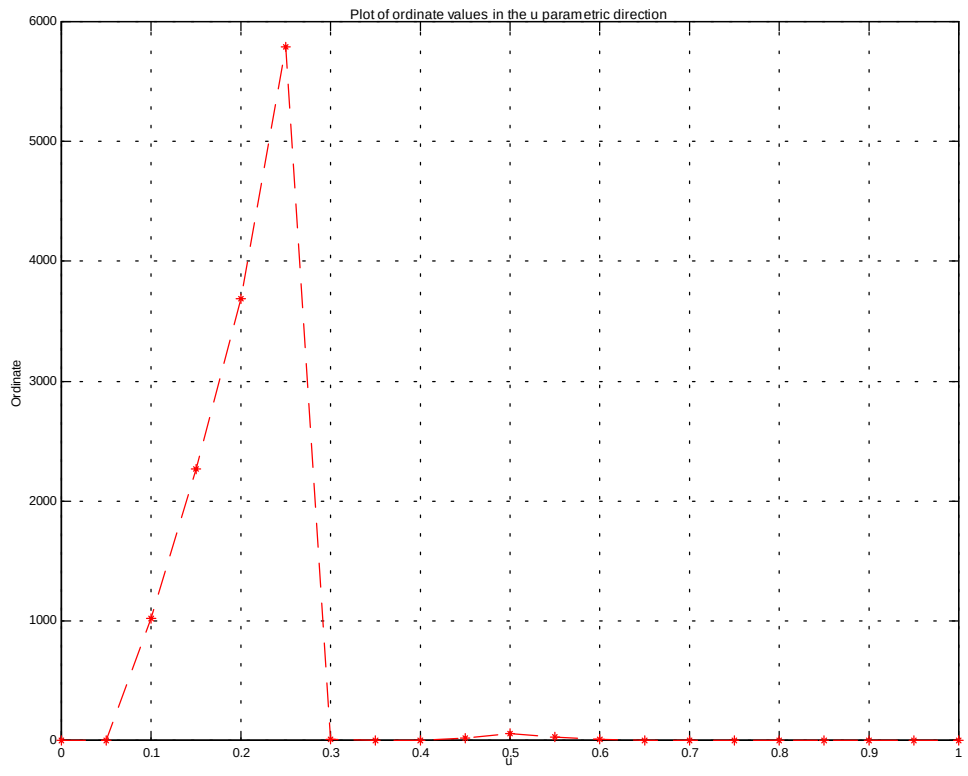

Figure 7.46: Case (vii) - Ordinate plot obtained after reducing the data for difference in radii of curvature for the original and matching surface. The radius of curvature is calculated for curves at regular isoparametric intervals in the u direction.

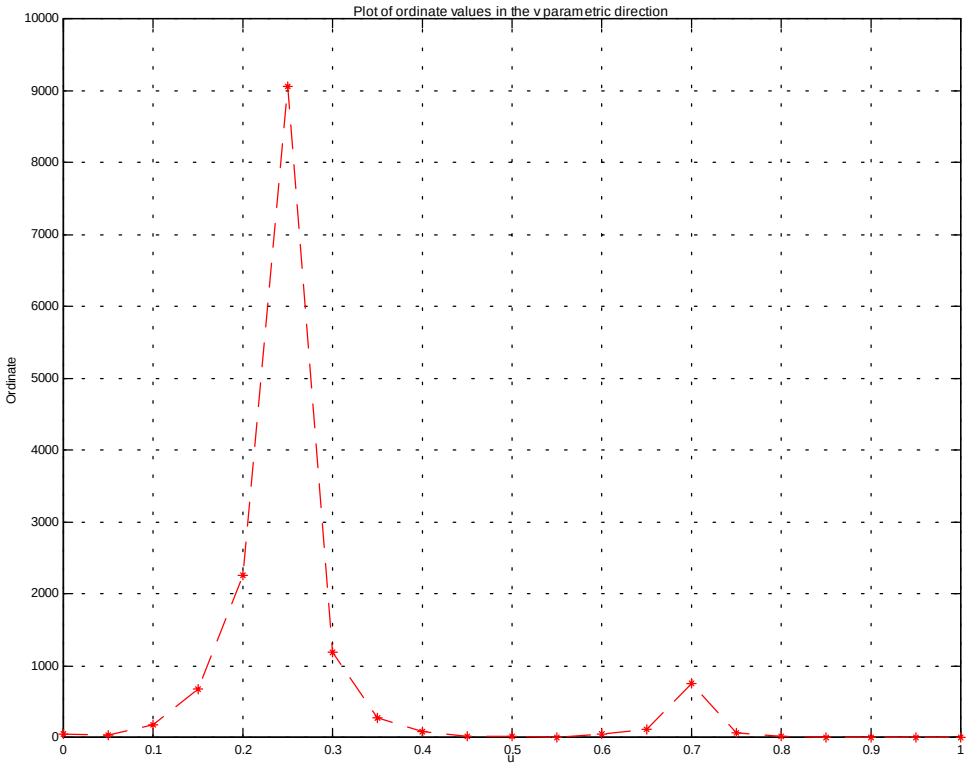

Figure 7.47: Case (vii) - Ordinate plot obtained after reducing the data for difference in radii of curvature for the original and matching surface. The radius of curvature is calculated for curves at regular isoparametric intervals in the v direction

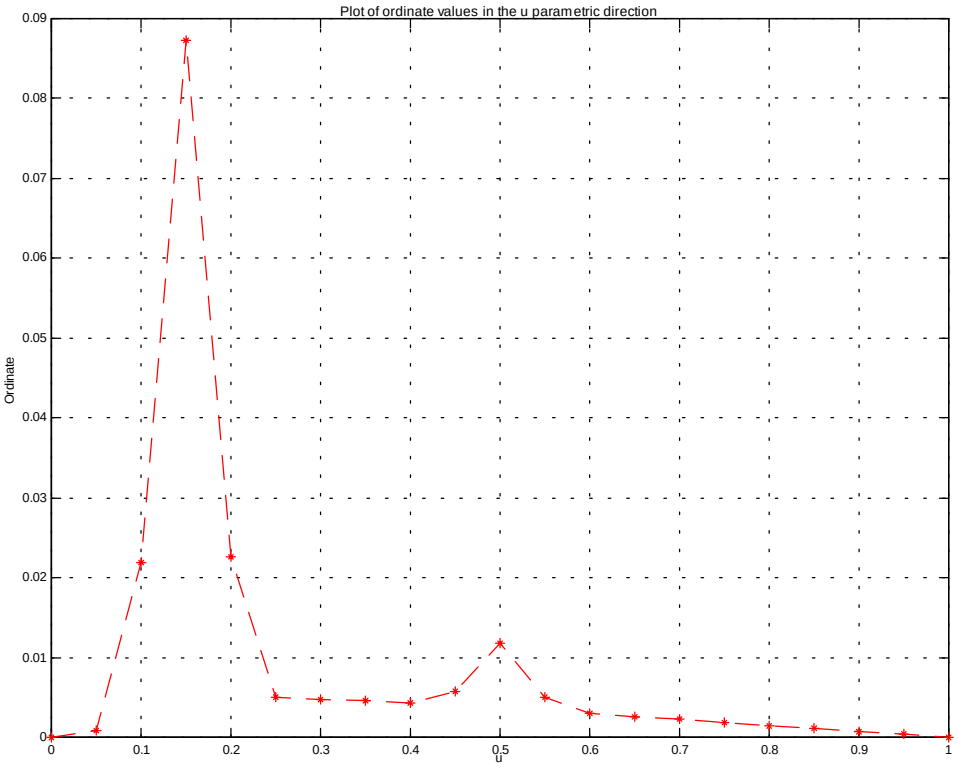

Figure 7.48: Case (vii) - Ordinate values for position error between the two surfaces along u direction.

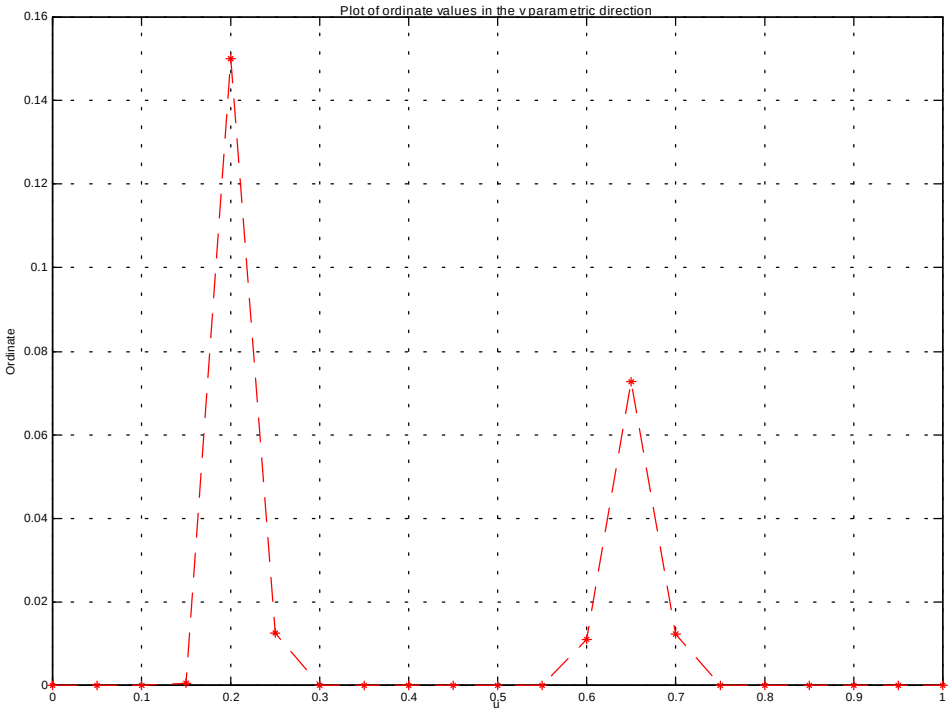

Figure 7.49: Case (vii) - Ordinate plot for position discrepancy data along v direction. This information is shown for comparison purposes.